Measurement: Energy 10 (2026) 100102

Contents lists available at ScienceDirect

Measurement: Energy

journal homepage: www.sciencedirect.com/journal/measurement-energy

Regular Paper

An optimized edge-assisted control system for low inertia photovoltaic microgrids in a cloud coordinating environment

Yiizzan Suffian [a], Ahmed M.A. Haidar [a,b,*], Tony Ahfock [b]

[a] Department of Electrical and Electronic Engineering, Universiti Malaysia Sarawak, Kota Samarahan, Sarawak, Malaysia
[b] School of Science, Engineering and Digital Technologies, University of Southern Queensland, Toowoomba, QLD, Australia

ARTICLE INFO

Keywords:
Edge computing
Grid-forming inverter
Controller-in-the-loop
Low-inertia system
Real-time monitoring system
Internet of things

ABSTRACT

The increasing integration of inverter-based resources such as solar photovoltaic is reshaping modern power systems, leading to a significant reduction in system inertia. This transition introduces challenges to both frequency and voltage stability, especially during faults and dynamic loads. To overcome these limitations, this paper proposes an optimized framework based on edge computing and a cloud-based coordination environment for virtual inertia support. Unlike conventional droop control methods, the proposed control strategy involves dynamically optimizing the control gains to minimize voltage and frequency fluctuations. Specifically, the proportional-integral-derivative (PID) parameters for both the frequency and voltage control loops within a droop control system are adjusted using a multi-objective particle swarm optimization (MOPSO) approach. The goal of this tuning is to enhance the system's ability to support inertia and improve its overall transient response characteristics. The control management system combines a local cloud node for real-time data exchange and oversight, allowing the optimizer to adjust system parameters to emulate the inertia characteristics of traditional synchronous machines. The controller is deployed on an embedded system, connected to a Synology network-attached storage (NAS) through the Internet of Things (IoT) for edge processing and data synchronization. A controller-in-the-loop (CIL) experimental setup has been developed to test and validate system performance under various operating conditions. This proposed approach significantly reduces voltage overshoot and keeps frequency deviation within a narrow range. Specifically, the hybrid algorithm achieves a 47% reduction in post-fault voltage overshoot and confines frequency deviation to within ±0.015 Hz. Additionally, it achieves a settling time of under 200 ms during severe disturbances. The timing performance demonstrates a latency of approximately 1 s per cycle, without compromising frequency or voltage stability.

1. Introduction

The widespread deployment of inverter-based resources, such as solar photovoltaics, battery systems, and hydrogen fuel cells, is rapidly transforming the structure and dynamics of modern power systems. As traditional synchronous machines are gradually phased out, the overall system inertia has significantly reduced, thereby weakening the grid's inherent ability to resist frequency and voltage disturbances [1]. This issue is particularly pronounced in microgrids with high renewable energy penetration, where low inertia significantly worsens power system stability during fault or transient events [2,3]. Grid-Forming (GFM) inverters are power electronic devices designed to mimic the behavior of traditional synchronous generators. They play a vital role in providing frequency and voltage support to the electricity grid. Unlike conventional grid-following inverters, which rely on an existing grid reference to operate, GFM inverters can function independently. They establish the grid's voltage and frequency, which significantly enhances overall system stability and resilience. Conventional droop control is widely used as a GFM control strategy because it is simple and decentralized; however, it has drawbacks such as poor dynamic performance and an inability to provide a robust inertial response for rapid frequency stabilization [4,5]. Recent work has introduced a hybrid droop-VSG and control system to improve transient stability by injecting inertia and adaptive damping [6–9]. Although these methods enhance response speed, many rely on real-time derivative estimation or high-bandwidth measurement systems, which leads to increased noise sensitivity and

* Corresponding author. UNIMAS, Department of Electrical and Electronic Engineering, Universiti Malaysia Sarawak, Jln Datuk Mohammad Musa, 94300, Kota Samarahan, Malaysia.
E-mail addresses: ahahmed@unimas.my, ahmed.haidar@unisq.edu.au (A.M.A. Haidar).

https://doi.org/10.1016/j.meaene.2026.100102
Received 6 October 2025; Received in revised form 18 April 2026; Accepted 29 April 2026
Available online 30 April 2026

computational burden [1]. Additionally, existing virtual inertia methods based on swing equations emulation are too complex for real-time implementation due to their reliance on derivative calculations and high-fidelity measurement systems [10]. These limitations motivate the integration of adaptive control techniques and embedded optimization strategies that can dynamically respond to system changes [11]. In this context, multi-objective optimization has emerged as a powerful technique to enhance frequency and voltage performance. Optimizing droop parameters and inertia emulation gains through multi-objective optimization enhances microgrid stability, resulting in improved damping of oscillations, faster dynamic responses, and superior voltage and frequency recovery under varying conditions. A common limitation in the existing literature is the tendency to optimize these methods using only a single objective function. Furthermore, most studies validate their optimization results solely through simulations, lacking crucial real-time experimental verification and analysis of communication-aware disturbances.

The advancement of emerging technologies, such as cloud-based supervisory control and the IoT, has enabled remote coordination and data-driven decision-making across distributed energy resources. The cloud platform allows for real-time performance monitoring, adaptive control, and effective energy coordination by interconnecting control hardware and grid simulations over secure wireless channels. Although heuristic optimization methods have shown promising results for smart grid control, previous research often lacked real-time validation under realistic conditions [12]. Cloud and edge computing present new opportunities for intelligent microgrid management. In this context, cloud platforms offer scalable data processing and global coordination, while edge computing facilitates faster localized decision-making. The strength of edge computing lies in its ability to reduce latency and offload computations from centralized systems, making it particularly suitable for time-sensitive smart grid control [13]. Edge computing provides significant advantages for inertia emulation in power systems by greatly reducing control loop latency. This reduction allows for a quicker frequency response and enhances overall grid stability. Such rapid responses are crucial for effectively managing the frequent fluctuations in frequency that are common in modern low-inertia grids with high levels of renewable energy integration [14]. Hence, the primary objective of this paper is to propose a control framework that is cloud-coordinated and edge-assisted. In this framework, a controller fine-tuned using the MOPSO algorithm is implemented on an embedded ESP32 platform. This platform connects to a local cloud node to enable faster data exchange and improved supervisory coordination. To validate the system, an experimental setup for CIL testing has been developed. This setup integrates Simulink-based microgrid modeling with real communication delays and embedded execution.

2. Review of related studies

A foundational technique in GFM control is conventional droop control, which enables decentralized power sharing among inverters by managing voltage and frequency based on active and reactive power deviations. While effective for steady-state sharing, droop control alone is insufficient for a fast-transient response. Its static nature means it cannot mimic the inertial characteristics of traditional rotating machines, leading to large overshoots and slow recovery during dynamic disturbances. Numerous studies have proposed the use of virtual synchronous generators (VSGs) and virtual inertia approaches to enhance the dynamic stability of low-inertia microgrids. These methods aim to replicate the swing dynamics of synchronous machines by injecting artificial inertia and damping into the control loop, which improves both active and reactive power management and strengthens frequency-voltage stability [7–9]. Authors in Ref. [7] introduced a virtual-inertia-based hierarchical control scheme that accounts for communication delays, leading to improved damping and synchronization behavior. Similarly, virtual-inertia inverters are increasingly being adopted in modern power electronic-dominated grids to address frequency instability resulting from high renewable energy penetration [9]. Despite these advantages, such implementations often depend on real-time derivative estimations of power or frequency, which can introduce noise and necessitate high-performance digital signal processing hardware. This makes them unsuitable for lightweight embedded systems [15,16]. Additionally, as highlighted in Ref. [17], virtual inertia techniques may encounter scalability and coordination challenges, motivating the development of optimization strategies to ensure their effectiveness, particularly in highly distributed networks.

To enhance droop and VSG performance, intelligent optimization algorithms such as particle swarm optimization (PSO), genetic algorithms, and fuzzy logic controllers have been employed to adaptively tune controller gains [6], [18]. These methods facilitate dynamic response adjustments, improving frequency damping, minimizing overshoot, and reducing settling times. For example, PSO is widely utilized due to its simplicity, rapid convergence, and effectiveness in navigating nonlinear search spaces [19]. However, many of these implementations focus solely on a single control objective, such as frequency deviation, while overlooking the effects on voltage stability or settling time. Recent studies have explored advanced control strategies and cloud integration to optimize the performance of smart grids. For instance, intelligent algorithms such as machine learning and fuzzy logic have been developed for optimal control decision-making through local historical data exchanged via cloud systems [20], [21]. In this context, PSO has been applied to fine-tune fuzzy controllers, leading to improved error minimization and energy management. Nonetheless, these studies often lack real-time implementation in complex grid scenarios and do not incorporate a diverse range of artificial intelligence techniques.

Authors in Ref. [12] proposed a hybrid private cloud framework to ensure secure data storage from power grid operations, using wireless sensor networks for monitoring. Similarly [22], emphasized the crucial role of IoT in multi-level utility data management and in shaping the concept of energy internet. Protecting sensitive information while enabling flexible data sharing is particularly useful in areas such as IoT and cloud environments. In this regard, the study in Ref. [23] developed an efficient and secure data acquisition scheme using a ciphertext policy attribute-based encryption for cloud-supported IoT in smart grid. Reference [24] defines the conceptual hierarchy of energy system terminologies, ranging from the broad “energy cloud” to the more specific

Table 1
List of abbreviations.

Abbreviation	Meaning
CIL	Controller-in-the-Loop
DER	Distributed Energy Resource
DRL	Deep Reinforcement Learning
EMS	Energy Management System
ESP32	Espressif 32-bit Microcontroller
F28335	Texas Instruments TMS320F28335 DSP
GFM	Grid-Forming
HIL	Hardware-in-the-Loop
HTTP	Hypertext Transfer Protocol
IoT	Internet of Things
MOPSO	Multi-Objective Particle Swarm Optimization
NAS	Network-Attached Storage
PCC	Point of Common Coupling
PID	Proportional–Integral–Derivative
PSO	Particle Swarm Optimization
PWM	Pulse Width Modulation
ST	settling time
SLDRT	Simulink Desktop Real-Time
SOC	State of Charge
VOC	Virtual Oscillator Control
VSG	Virtual Synchronous Generator
VSM	Virtual Synchronous Machine
GDC	Generalized Droop Controller
EW	Existing work
RTDS	Real Time Digital Simulator

Table 2
Comparison of previous studies with the existing work (EW) in terms of advantages and limitations.

Ref.	Control approach	Cloud/Edge integration	Key advantages	Key limitations
[1]	Optimized Universal Droop Control Framework	Droop Control via MATLAB integration (cloud-like optimization)	Fault localization, low latency, resilient load support	Computationally heavy, lacks embedded/edge deployment
[4]	PSO-based droop control in steady state and partial load conditions	None	Enhance the efficiency of the system by reducing inverter and transmission losses	Did not consider frequency and voltage stability
[10]	Traditional rule-based EMS for networked DC microgrid	Communication layer for edge coordination	Real hardware implementation with low latency demonstrates resiliency and stable power-sharing	Computational complexity of the algorithm
[12]	Private hybrid cloud for grid monitoring	Application of a smart meter via a local area network	Secure communication via wireless sensor networks	Lacks edge decision-making and real-time tuning
[22]	IoT-enabled smart grid coordination without optimization	Internet of Things (smart meter)	Utility-level scalability	Latency and security concerns, no edge deployment
[20]	Machine learning-based VSG with fuzzy rule sets	Cloud operation scheme for cooperative information exchange	Adaptive control using historical datasets	No real-time control or HIL or CIL validation
[29]	Edge-based multi-agent reinforcement learning for energy management	Edge-integrated deep reinforcement learning	Fast, scalable, DRL-coordinated	No inertia emulation
[32]	Event-triggered rule-based voltage edge control	Edge device and cloud Applications as control commands for monitoring purposes	Low latency	No MOPSO tuning
[33]	Deep reinforcement learning with edge computing	None	Local decision-making with global learning	High training cost, lacks embedded HIL validation
EW	MOPSO tuned droop and virtual inertia control	Application of ESP32 and F28335 microcontrollers in edge cloud computing	Robust cybersecurity features to prevent unauthorized access and ensure system integrity	Fully embedded CIL simulation with simultaneous frequency–voltage optimization

"energy hub". The first addresses all physical and virtual electric system infrastructure, while the second focuses on localized, internet-connected physical infrastructure, with smart energy, energy internet, and transactive energy in between. In Ref. [25], the authors proposed a secure signal extraction method for a low-frequency control system against false data injection attacks, considering a real multi-channel feature of the power communication network. Integrating an IoT-enabled data acquisition system could enhance the dynamic response of such systems, allowing for robust cybersecurity features to prevent unauthorized access and ensure system integrity. With the integration of renewable energy resources, transferring large datasets through information and communications technology infrastructure increases complexity for utility operators in the power system. Therefore, recent studies started focusing on cloud-based supervisory systems and virtual machine coordination for smart grids, but with less effort on edge-assisted GFM control, particularly with CIL integration. It is worth mentioning that the data volume in smart grids is forecasted to increase sharply in the future, underscoring the need for efficient edge-cloud coordination [26]. (see Table 1 for a list of abbreviations).

Efficient edge-cloud coordination is crucial for leveraging the complementary strengths of both edge and cloud computing to enable real-time smart grid operations [27], [28], allowing for real-time processing with low latency and high bandwidth while still leveraging the power of the cloud for heavier tasks [29]. Cloud-edge coordinated energy management systems (EMS) proposed in Ref. [30] further enable two-way communication between utilities and smart hubs, ensuring cost-efficiency, flexibility, and intelligent load balancing. The authors in Ref. [31] successfully demonstrated parallel power flow calculation on a large-scale power system using Spark on a cloud computing platform, achieving good performance. However, they noted that the advantages of this approach are less apparent on a smaller test system. Recent advancements in edge computing have started to transform the landscape of smart grid control, particularly in enabling fast, localized decisions at the device level while maintaining coordination with cloud supervisory layers. For instance, Ref. [29] introduced an edge-enabled deep reinforcement learning (DRL) framework that optimizes power flow in microgrids through distribution. This structure accelerates control response by processing measurements locally while leveraging the cloud for training and policy updates. Similarly, the authors in Ref. [32] implemented a hybrid control system based on event-triggered mechanisms within edge networks. The study demonstrated significant latency reductions and resilience against cyber-physical disruptions by executing rule-based voltage control directly on edge devices without integrating optimization mechanisms. The study in Ref. [33] proposed a multi-agent DRL-based cooperative energy management system that combines edge inference with global learning models to enable active demand-side management by embedding intelligence at the regional level. While the design in Ref. [33] is conceptually sound, the implementation lacked CIL experimental validation and neglected inertia emulation or multi-objective tuning. The literature gap is addressed through a comparative analysis presented in Table 2, which reviews previous studies with a focus on control topology, optimization methods, and system integration, with their respective advantages and limitations. As detailed in Table 2, the majority of earlier studies primarily focused on single-domain enhancements. For instance, research such as [12] and [20] introduced intelligent control systems or secure cloud-based monitoring solutions. However, these efforts did not incorporate real-time validation or embedded execution. Similarly, other investigations, including [29] and [33], explored virtualization or reinforcement learning for load balancing, but they resulted in considerable computational overhead and did not involve implementing controllers on physical hardware.

The study in Ref. [34], which utilized a PSO-tuned droop controller for a microgrid, is limited by the Arduino hardware and communication infrastructure it relied on. Existing studies [1,4,10,12,20,22,29,32,33] also share shortcomings, such as focusing on a single optimization objective, not testing algorithms in a real-time embedded environment, or failing to include inertia emulation in edge-deployable PID controllers. This study presents an innovative approach by incorporating a fully adjustable edge controller that employs a dual-PID and droop control algorithm with the ESP32 platform. The effectiveness of this approach is validated through CIL scenarios. Additionally, the integration of the MOPSO algorithm for tuning droop parameters in a cloud-coordinated environment can effectively minimize deviations in both frequency and voltage. This allows the entire system to replicate the dynamic behavior of inertia without the need for extensive computational resources. The scope of this work is to develop a fully functional edge-cloud hybrid framework for real-time control, utilizing MOPSO to optimize droop and PID parameters. The system ensures low-latency performance by using an ESP32 as an edge controller, with a Synology NAS providing reliable cloud-based data logging and supervisory control. Furthermore, the proposed controller employs innovative

Table 3
Performance benchmarking of the proposed MOPSO-PID controller against GFM alternatives.

Control scheme	Main principle	Strength	Drawbacks	Embedded/edge suitability
Conventional droop	Static P–f/Q–V regulation	Simple, decentralized	Weak inertia emulation, slower transient response	High
VSM	Emulates synchronous machine swing dynamics	Strong inertia-like behavior, intuitive physical analogy	Higher computational complexity, derivative/ state dependence, heavier implementation	Medium
VOC	Oscillator-based synchronization and control	Fast synchronization, strong nonlinear dynamic behavior	More complex design and parameterization for the present low-cost architecture	Medium
Proposed MOPSO-tuned droop-PID	Optimized droop with dual PID adaptation	Improved damping and recovery with lower implementation burden	Does not claim universal superiority over all GFM schemes	High

gain-adaptive control on the F28335 microcontroller to emulate inertia, eliminating the need for computationally intensive swing equation models. This approach substantially reduces processing requirements, making the system suitable for resource-constrained devices and demonstrating a practical, robust approach to microgrid testing via CIL integration with Simulink under fault and dynamic loading conditions. Unlike the previous studies summarized in Table 2, which primarily focused on traditional droop control or limited hybrid control

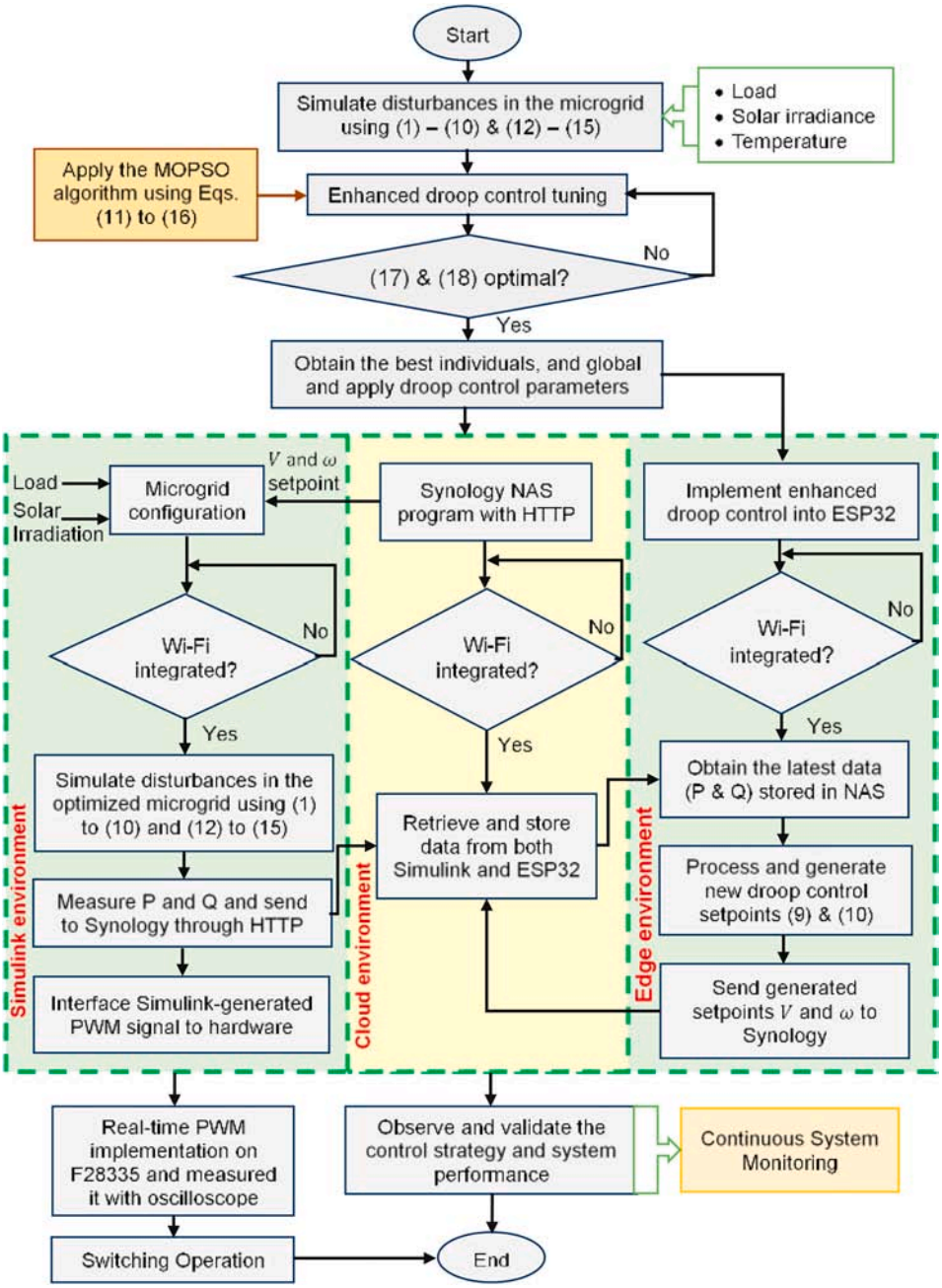

Fig. 1. Hybrid algorithm for low-inertia microgrids.

algorithms, this research integrates optimization techniques, embedded systems, and coordinated control. The goal is to achieve effective stabilization of low-inertia microgrids through the application of virtual inertia techniques within a real-time CIL simulation environment. The proposed system features a grid-integrated microgrid that incorporates real-time IoT-based condition monitoring. Specifically, this paper bridges the gap between theoretical virtual inertia control and its practical implementation on physical hardware for microgrids characterized by low inertia and high renewable energy penetration. The primary contributions of this work are as follows:

- Formulating a modeling approach capable of stabilizing both frequency and voltage deviations within a narrow range.
- Developing a coordinating system utilizing a local cloud node to enhance data exchange and supervisory control for inertia support in grid-integrated microgrids
- Establishing a controller-in-the-loop experimental setup for low-latency operation validation to ensure synchronized system coordination with physical controllers.

The purpose of the present work in this paper is not to claim universal superiority over all GFM schemes. Instead, the main contribution is to demonstrate that an optimization-assisted droop-based architecture can provide effective frequency-voltage stabilization while remaining computationally lightweight and suitable for edge implementation. This positioning is especially relevant for low-cost embedded controllers and cloud-coordinated microgrid applications. Unlike conventional VSM methods, this approach removes the need for explicit swing-equation emulation and derivative-dependent states, significantly reducing computational load for resource-constrained hardware. Furthermore, it maintains a simpler, droop-based structure compared to VOC, aligning better with conventional power-sharing and practical tuning. While VSM and VOC offer strong dynamic performance, a direct experimental benchmark is beyond this study's scope. Although VSM and VOC provide superior dynamic performance, direct experimental benchmarking is outside the scope of this study. Beyond the study-level comparison in Table 2, Table 3 qualitatively positions the proposed method against representative grid-forming families, specifically droop, VSM, and VOC, to clarify its practical niche. As detailed in Table 3, the proposed method enhances transient support and damping over conventional droop while maintaining a lower computational burden than complex dynamic-emulation schemes. This makes the controller suitable for resource-constrained edge platforms and cloud-coordinated microgrids.

This study begins with an introduction in Section 1 that emphasizes its importance. Following this, the literature review identifies the research gap and justifies the contributions of the study. The rest of the paper is organized as follows: Section 3 provides a detailed explanation of the edge-assisted framework for low-inertia microgrids and the hardware implementation. This section covers virtual inertia emulation through an adaptive MOPSO-based control system for a cloud-coordinated microgrid, including the optimized edge-assisted control in a cloud environment. In Section 4, the results obtained from various simulation scenarios are presented, accompanied by extensive evaluation and analysis to validate the robustness of the proposed approach. Detailed results from the Synology real-time monitoring system are also discussed, which include the operating signals from all hardware controllers. Finally, Section 5 summarizes the main findings, highlights the significance of this research, and suggests directions for future studies to address existing limitations.

3. Edge-assisted framework for low-inertia microgrids

This section outlines an edge-assisted framework integrated with optimized droop control for low-inertia microgrids, particularly in a cloud-coordinated environment. The hybrid algorithm for low-inertia microgrids, illustrated in Fig. 1, combines edge computing for local control actions with cloud computing for overall coordination. This integration enhances stability and resilience. The improved droop control strategies effectively manage power flow and regulate voltage with frequency in low-inertia systems, where traditional droop control methods may face challenges. The control system is designed to emulate virtual inertia using the MOPSO approach, implemented in real-time on the ESP32-based edge controller and the F28335-based cloud controller. In this step, the controllers utilize a local cloud node as a central hub for exchanging data and implementing supervisory adjustments. This means that the controller is embedded on an ESP32-based edge computing platform, while supervisory coordination and data storage are handled by a Synology NAS, acting as a local cloud node. The microgrid is modelled in Simulink and continuously exchanges active and reactive power data with the F28335 controller over Hypertext Transfer Protocol (HTTP). Control decisions are computed at the edge using real-time data, while the cloud provides supervisory logic and periodic adjustments. Decentralizing control in a grid-connected microgrid enhances efficiency and responsiveness. This strategy creates a more robust system by distributing management and decision-making authority, resulting in lower latency, better scalability, and improved fault tolerance [13]. Referring to Fig. 1, which comprises three core layers, the microgrid is modelled with dynamic loads and renewable energy resources. Here, the optimized control algorithm is distributed between the simulated microgrid plant, the embedded edge controllers, and the local cloud-based supervisory management system. Unlike traditional virtual inertia techniques that rely on differential modeling, the proposed method emulates inertia by using dynamically optimized PID and droop gain scheduling, which is tuned using the MOPSO algorithm. This approach simultaneously minimizes frequency and voltage deviations while ensuring short settling times. The system's effectiveness is validated through CIL testing under various fault conditions. The following subsections present the modelling of the edge-assisted framework, elaborating on the decentralized control strategy and the optimized control algorithm for gain tuning. The next steps involved designing the cloud coordination system, which is implemented using a local node and the test system's hardware.

3.1. Virtual inertia emulation through optimized droop tuning

Generally, unoptimized droop control is a common GFM control approach in which the inverter regulates frequency and voltage in response to power imbalances [8]. This method permits GFM inverters to operate independently in off-grid or weak-grid conditions by emulating the behavior of traditional synchronous generators. The static droop relationships are expressed in Eqs. (1) and (2) [35] where ω and ω_{ref} signify actual and nominal angular frequencies, while V *and* V_{ref} are the actual and nominal voltages. M and D represent the droop gains for frequency and voltage, respectively. Inertial control in the microgrid, specifically virtual inertia, uses gain values and reference values, active and reactive values P_{ref} and Q_{ref}, to adjust a system's output in response to changes in active and reactive power. This control strategy aims to replicate the inertial response of traditional synchronous generators, particularly those with high penetration of renewable energy sources [9]. The conventional virtual inertia control utilizes differential equations that include explicit terms representing virtual inertia and damping. Equations (3) and (4) incorporate the rate of change of angular frequency $\frac{d\omega}{dt}$ and voltage $\frac{dV}{dt}$ alongside virtual inertia constant J and virtual damping coefficient C [8], [36]. These terms effectively mimic the behavior of a synchronous machine's inertia and damping characteristics within power systems. However, real-time implementation of $\frac{d\omega}{dt}$ and $\frac{dV}{dt}$ can be computationally expensive, leading to delays and limited performance. Furthermore, noise sensitivity in these calculations can introduce inaccuracies, and hardware limitations can restrict the speed and complexity of the computations that can be performed in real-time [36], [37]. The proposed controller does not explicitly model virtual

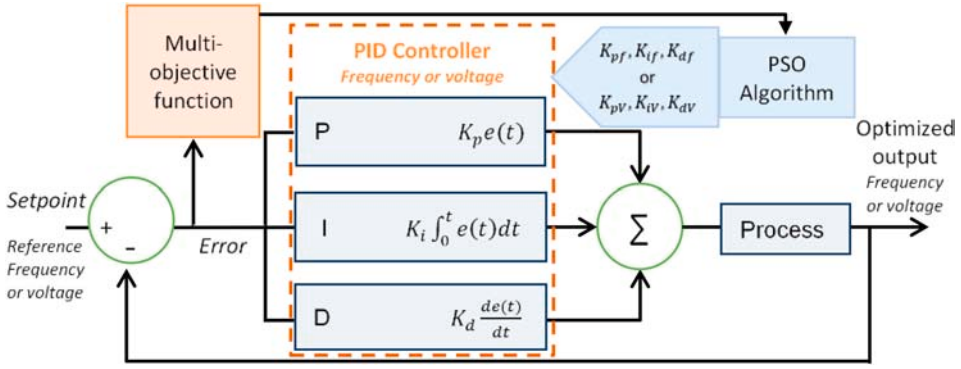

Fig. 2. Optimized PID controller structure for frequency or voltage.

torque or swing dynamics. Instead, it emulates inertia by adaptively adjusting droop-based frequency and voltage regulation gains. In this framework, the PID parameters are used to modulate the effective stiffness and damping of the control loop. By increasing the proportional and derivative actions, the controller enhances its ability to respond to sudden deviations, thereby creating a functional equivalent of an inertial torque response without the need to compute explicit derivatives. This approach aligns with recent studies demonstrating that optimized PID-supervised droop control enhances damping, decreases overshoot, and speeds up settling time characteristics typically linked to the behavior of virtual inertia [38], [39]. These techniques have been successfully used in adaptive PSO droop controllers and auto-tuned droop-based microgrid systems. Both types of systems have shown that gain adaptation can improve transient stability in a way similar to virtual inertia injection. Consequently, this study proposes an integrated edge-and-cloud computing approach to address the unique management challenges of low-inertia microgrids.

$$\omega = \omega_{ref} - M(P - P_{ref}) \tag{1}$$

$$V = V_{ref} - D(Q - Q_{ref}) \tag{2}$$

$$\omega = \omega_{ref} - M(P - P_{ref}) - J\frac{d\omega}{dt} \tag{3}$$

$$V = V - D(Q - Q_{ref}) - C\frac{dV}{dt} \tag{4}$$

The proposed method enhances conventional static droop equations by integrating two independent, optimized PID controllers. One controller is dedicated to the frequency/active power, while the other handles the voltage/reactive power loop, improving stability and power sharing accuracy. This approach deviates from dynamic differential modeling by directly modifying the static droop characteristics. In this sense, the enhanced MOPSO algorithm presented in the next subsection is employed to concurrently determine optimal values for specific control parameters "K_{pf}, K_{if}, K_{df}" for frequency control and "K_{pV}, K_{iV}, K_{dV}" for voltage control. Thus, the inverter-based resources, with optimized control strategies, can mimic the dynamic behavior of inertia and damping, traditionally associated with synchronous generators. This virtual inertia is achieved by dynamically adjusting the control gains of the inverter, effectively emulating the inertia and damping characteristics of a synchronous machine, rather than relying on physical inertia. The final output of the control system, described by Eqs. (9) and (10) are derived from a combination of droop control and the contributions of proportional (P), integral (I), and derivative (D) control actions, as illustrated in Fig. 2 and detailed in Eqs. (3)–(8). Where $e_P(t)$ and $e_Q(t)$ are active and reactive power errors, and K_p, K_i, K_d are the PID gains for each control loop.

$$e_P(t) = P_{ref} - P(t) \tag{5}$$

$$e_Q(t) = Q_{ref} - Q(t) \tag{6}$$

$$PID_f\ (e_P) = K_{pf}e_P(t) + K_{if}\int e_P(t)dt + K_{df}\frac{de_P(t)}{dt} \tag{7}$$

$$PID_V(e_Q) = K_{pV}e_Q(t) + K_{iV}\int e_Q(t)dt + K_{dV}\frac{de_Q(t)}{dt} \tag{8}$$

$$\omega = \omega_{ref} - M(e_P)(PID_f) \tag{9}$$

$$V = V_{ref} - D(e_Q)(PIV_V) \tag{10}$$

3.2. Adaptive MOPSO-based edge-assisted control for cloud-coordinated microgrid

The study utilizes Particle Swarm Optimization (PSO), a problem-independent metaheuristic chosen for its ability to navigate complex, uncertain search spaces with few assumptions. To handle the specific requirements of the microgrid, it is implemented as a multi-objective technique that balances competing performance metrics rather than a single goal. The Algorithm: Hybrid Edge-Assisted Optimization. The proposed algorithm integrates MOPSO into a hybrid control architecture to enhance conventional droop control. Its core components include:

Pre-real-time tuning: The algorithm tunes PID gains in advance to enhance responsiveness and ensure robustness against faults or load fluctuations.

Enhanced Constraints: The standard PSO is modified by incorporating settling time (ST) as a conditional value within the multi-objective framework.

Objective Function: The algorithm seeks to minimize three primary variables: frequency deviations, voltage deviations, and settling time.

Operational Context: The optimization is subject to constraints involving total power generation, grid power exchange (import/export), energy storage levels, and total load demand.

When selecting an optimization technique, the complexity of the problem and the associated computational cost are indeed crucial factors to consider. While some methods guarantee global optima, they might be computationally expensive. Heuristic methods, despite not always finding the absolute best solution, often provide good enough results within reasonable computational limits. The PSO is a problem-independent metaheuristic, making it suitable for a wide range of optimization problems compared to a problem-specific heuristic. Its advantage lies in requiring fewer assumptions when searching for solutions in complex, uncertain spaces, which can lead to faster convergence towards optimal or near-optimal solutions [40]. Therefore, PSO is chosen in this study as an optimization component in the proposed hybrid algorithm. The standard PSO is further enhanced by incorporating a settling time (ST) as a conditional value with a multi-objective function, creating an effective hybrid edge-assisted optimized

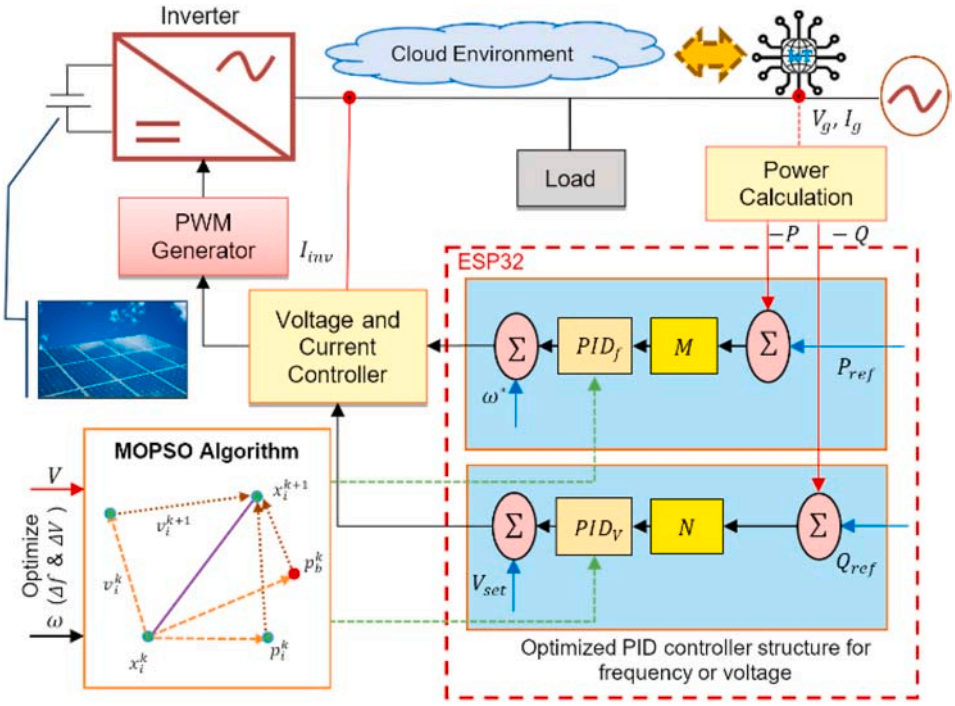

Fig. 3. Integration of edge-cloud optimized droop control.

algorithm. The control architecture described in Fig. 3 combines the simplicity of conventional droop control with enhanced dynamic responsiveness through real-time PID adaptation. This is achieved by optimizing all PID gains using MOPSO, making the controller robust against various fault conditions and load changes. In this sense, the objective function in (11) aims to minimize frequency and voltage deviations, as well as settling time, by adjusting controller gains through PID tuning of parameters subjected to some constraints given in (12) – (15). Where $P_{MG}(t)$ is the total power generation in the microgrid at time "t"; $\pm P_{PG}(t)$ is the imported or exported power to the grid; $\pm P_{ES}$ represents the energy storage; $P_i^L(t)$ is the total load demand.

Table 4
Parameter settings employed in the MOPSO algorithm.

Category	Parameter	Acronym	Allowed tolerance
Weighting/ Scaling	Frequency deviation weighting	w_f	1 (implicit through ±5% constraint band)
	Voltage deviation weighting	w_V	1 (implicit through ±5% constraint band)
Inertia Weight Schedule	Initial inertia	w_0	0.9
	Final inertia	w_1	0.4
PSO Coefficients	Inertia update	w^k	—
	Cognitive coefficient	c_1	2
	Social coefficient	c_2	2
	Random terms	r_1, r_2	0,1
Optimization Variables	PID gains (frequency loop)	K_{pf}, K_{if}, K_{df}	[0–5], [0–5], [0–1]
	PID gains (voltage loop)	K_{pv}, K_{iv}, K_{dv}	[0–5], [0–5], [0–1]
Constraints	Frequency limit	f_{min}, f_{max}	±5% around 50 Hz
	Voltage limit	V_{min}, V_{max}	±5% around 240 V
	SOC constraint	SOC_{min}, SOC_{max}	20–80%)
Simulation Setup	Evaluation duration	—	10 s per iteration
	Swarm size	—	20 particles, 20 iterations

$$Minimize\left(\sum_t^T \Delta f + \sum_t^T \Delta V + \sum_t^T \Delta ST\right) \tag{11}$$

$$P(t) = P_{MG}(t) \pm P_{PG}(t) \pm P_{ES} - P_L(t), \forall\, t \in T \tag{12}$$

$$f_{min} \le f(t) \le f_{max} \tag{13}$$

$$V_{min} \le V(t) \le V_{max} \tag{14}$$

$$SOC_{min} \le SOC(t) \le SOC_{max} \tag{15}$$

The low-inertia control strategy uses the MOPSO to optimize the PID controller gains for frequency and voltage regulation. The MOPSO process begins by initializing a particle population, then iteratively updates the particle velocities "v_i" and positions "x_i" using Eq. (16) until a convergence criterion "k" is met, as indicated in the lower-left portion of Fig. 3. This iterative updating is the core of the PSO algorithm. The PID controller gains in a Simulink-based microgrid model are optimized by applying them iteratively to the mathematical model represented by equations from (3) to (10), along with disturbance scenarios. The optimization process defined by Eq. (11) aims to find the best PID parameters that minimize the voltage and frequency deviations from the desired operating points and reduce settling time during disturbances. Specifically, the algorithm searches for the best individuals "p_i^k" and the best global "p_b^k" parameter settings as expressed in Eqs. (17) and (18). The system ensures that the grid's frequency and voltage return to their nominal levels. This involves using cognitive and social coefficients (c_1, c_2), uniformly distributed random values (r_1, r_2), and optimization functions to minimize deviations in frequency and voltage (Δf) and (ΔV), weighted by inertia (w_f, w_v) and penalized for errors (γ_f, γ_v). The momentum weight "w" is a crucial parameter that maintains the original speed and controls the balance between local and global search capabilities. Where w_0 and w_1 are the initial and final values of w; k and n are the current number of iterations and total number of iterations, respectively.

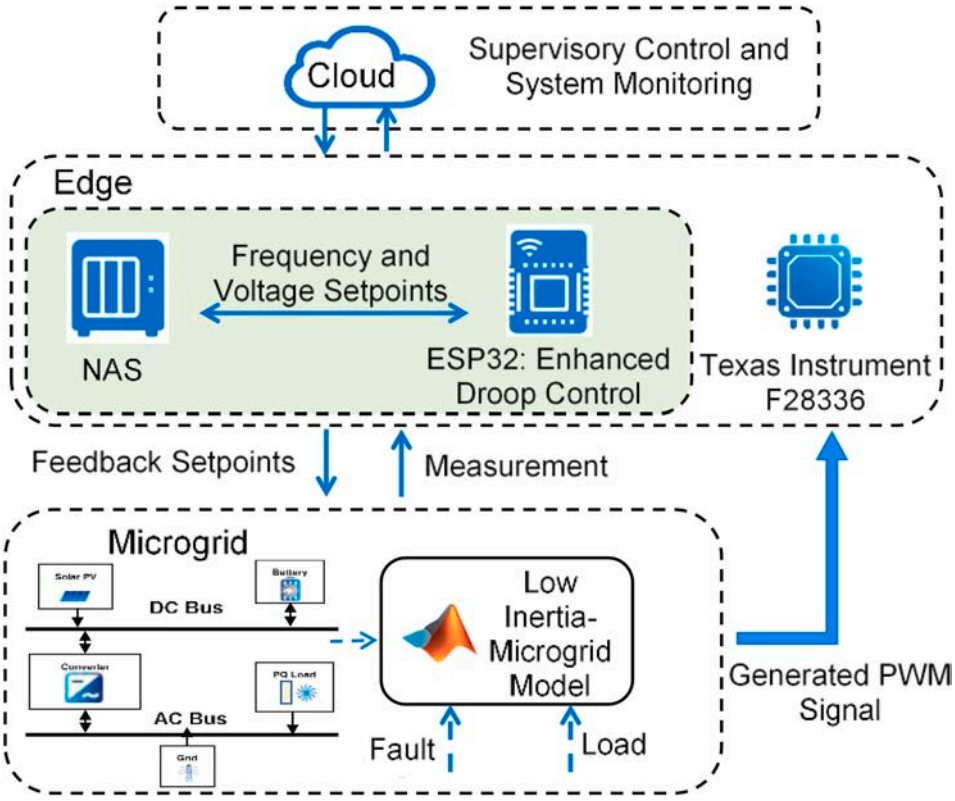

Fig. 4. Real-time cloud-edge hardware implementation.

$$v_i^{k+1} = wv_i^k + c_1 r_1 \left(p_i^k - x_i^k\right) + c_2 r_2 \left(p_b^k - x_i^k\right); \begin{cases} x_i = \left(K_{pf}, K_{if}, K_{df}, K_{pv}, K_{iv}, K_{dv}\right) \\ w^k = w_0 + (w_1 - w_0)\dfrac{k}{n} \\ x_i^{k+1} = x_i^k + v_i^{k+1} \end{cases} \tag{16}$$

$$\Delta f = \sum_{t=1}^{T} \left[w_f \left(f(t) - f_{ref} \right)^2 \right]; \begin{cases} \gamma_f, if\ \Delta f_{max} < \Delta f < \Delta f_{min} \\ 0, otherwise \end{cases} \tag{17}$$

$$\Delta V = \sum_{t=1}^{T} \left[w_V \left(V(t) - V_{ref} \right)^2 \right]; \begin{cases} \gamma_V, if\ \ \Delta V_{max} < \Delta V < \Delta V_{min} \\ 0, otherwise \end{cases} \tag{18}$$

The objective outlined in Eq. (11) aims to minimize cumulative frequency deviation, voltage deviation, and settling time. However, it is essential to understand that these deviations are normalized within the acceptable operating range defined by the constraints in Eqs. (13) and (14). This normalization ensures that frequency and voltage deviations remain within comparable numerical ranges, preventing any one term from dominating the others. Additionally, Eq. (16) has been expanded to explicitly include the formula for adapting the inertia weight. The inertia weight decreases linearly from w_0 to w_1 over the optimization horizon, promoting global exploration during the early iterations and local refinement in the later ones. The search boundaries for all PID controller gains are included to ensure feasibility and stability throughout the optimization process. Table 4 provides a comprehensive overview of the key parameters utilized in the MATLAB-based MOPSO implementation, which is integrated with the Simulink model. Specifically, the table summarizes the weighting factors, inertia weight formulation, and the boundaries for the PID parameters, reflecting the values employed in the actual simulation. Referring to Table 4, It is important to clarify that while ±5% is acceptable for microgrid operations, during severe disturbances such as three-phase faults, frequency deviations are evaluated against emergency or protection thresholds rather than continuous operation limits. In such emergencies, various sources indicate that protection ride-through thresholds can drop to around 47.5 Hz in 50 Hz systems [41], [42], [43]. The frequency range of 49 Hz to 51 Hz is generally considered the tolerance band for transient conditions in a 50 Hz power system, not the normal continuous operating range. For most 50 Hz grids, the typical normal operating frequency band for continuous and stable operation is much tighter, usually between 49.8 Hz and 50.2 Hz, or even narrower, such as 49.9 Hz to 50.05 Hz.

As shown in Fig. 3, the MOPSO algorithm is executed externally in the MATLAB/Simulink environment on the host PC during the offline tuning phase. The optimized parameters for the frequency and voltage PID loops are then transferred to the ESP32 controller. During online operation, the ESP32 executes the tuned droop-PID control law, while the Synology NAS serves as the communication and supervisory data hub. Consequently, the MOPSO algorithm is not executed on the ESP32 or the Synology NAS during the real-time closed-loop cycle.

After tuning the PID controller, the optimal parameters are implemented on the ESP32, which is part of the edge environment. As illustrated in Figs. 1 and 3, the system operates in a closed-loop configuration that integrates a Simulink environment (bottom left), a cloud environment (bottom middle), and the ESP32-based edge environment (bottom right). The primary component in this setup is the cloud environment, with a Synology NAS serving as the central data hub. This NAS utilizes HTTP protocols to synchronize data between the Simulink environment and the edge environment, effectively acting as a bridge for data exchange between the cloud and edge devices. In the edge layer of the overall algorithm, the ESP32 runs a tuned droop controller. This controller leverages the latest active and reactive power measurements retrieved from the real-time cloud data to adjust the setpoints for frequency "ω" and "V" using equations (9) and (10). Simultaneously, the pulse width modulation (PWM) waveforms generated by Simulink code running on the F28335 microcontroller can be measured with an oscilloscope to verify their frequency and duty cycle characteristics. The

enhanced MOPSO-tuned controller provides a straightforward, responsive, and computationally efficient method for managing power in low-inertia microgrids. By simultaneously optimizing droop gains and dual-droop PID parameters, the controller effectively simulates virtual inertia without requiring complex system modeling. This approach has been validated through both simulation and hardware testing, demonstrating its suitability for deployment on embedded systems in modern smart microgrids.

3.3. Real-time CIL platform for edge-cloud coordination

This section describes the CIL implementation of the optimized edge-assisted control within a cloud-coordinated environment. The hardware implementation outlined in Fig. 4 involves a five-stage process. The enhanced droop control strategy tuned using MOPSO is executed on an ESP32 edge device and coordinated via a cloud-based platform using the Synology drive and F28335 microcontroller. The system integrates a Simulink model of a microgrid with real-time embedded control and cloud-based data exchange, validating the effectiveness of controllers under realistic operating conditions. The primary objective is to evaluate the performance and practicality of the improved droop control method for a grid-connected microgrid, specifically when utilizing edge-cloud coordination for enhanced control capabilities. Initially, the microgrid model is simulated in the MATLAB Simulink environment to verify the effectiveness of the MOPSO-optimized controller. Once validated, the control algorithm is directly deployed to the ESP32 module, allowing real-time operation in edge-cloud coordination. The active and reactive power measurements from the simulation are transmitted to an ESP32 microcontroller via a Synology NAS. The ESP32 then utilizes this data to calculate the optimal voltage and frequency setpoints using the MOPSO-based droop control algorithm. The calculated setpoints are uploaded to the system for closed-loop control. The Texas Instruments F28335 microcontroller connected to a Simulink-generated closed-loop system is used to produce PWM signals. These signals can then be measured using an oscilloscope and also monitored using IoT analytics platforms like ThingSpeak, providing a way to verify the system's functionality and performance. This setup demonstrates the scalability and practicality of intelligent edge-cloud control in stabilizing frequency and voltage within a low-inertia microgrid. Referring to Fig. 4, the CIL platform for edge-cloud coordination comprises the following key steps in designing experimental work with the related components:

- The microgrid simulation system is configured to periodically transmit real-time power measurements, including active power (P), reactive power (Q), frequency (f), and voltage (V). This data transmission is facilitated by a custom script named "SendToSynologyHTTP.m".
- A Synology NAS device is designated as the data recipient, utilizing a PHP script called "write_data.php" to process, organize, and store the incoming measurements in comma-separated values (CSV) format. This setup enables the continuous collection and logging of critical operational parameters from the simulated microgrid into the centralized storage system.
- The ESP32 microcontroller interacts with a server-side script "read_data.php" to retrieve previously stored data. The optimized control logic of ESP32 then utilizes this data to calculate the optimal frequency and voltage reference outputs. The computed results are sent back to the server for storage and monitoring or future processing through another server-side script named "droopoutput.php" programmed in the NAS, thus enabling remote control, data logging, and dynamic system adjustments based on external inputs or predefined logic.
- The Simulink then interacts with external data sources by reading the reference values via "read droopoutput.php" and "ReceiveFromSynologyHTTP.m" and generates the PWM signals for inverter operation, closing the overall loop of the system. The real-time generated PWM signal is transmitted to the Texas Instruments F28335 microcontroller for measurement via oscilloscope to provide a visual representation of the PWM signal's characteristics, and this transmission occurs alongside the execution of a loop.

The pseudocode representations of the implemented procedures, particularly for the data exchange mechanisms between Simulink, the ESP32 controller, and the Synology NAS, are summarized below.

Pseudocode of the data exchange mechanisms

```
Initialize simulation parameters (V_ref, ω_ref, M, D, PID_f, PID_V)
Start Simulink microgrid model
  Loop while simulation is running:
  Measure P(t), Q(t) at PCC
  Call "SendToSynologyHTTP.m" (P(t), Q(t))
    On Synology NAS:
      "write_data.php" stores {timestamp, P(t), Q(t)} in CSV format
    On ESP32 controller:
      "read_data.php" retrieves latest P(t), Q(t)
      Compute ΔP, ΔQ relative to nominal frequency and voltage; 50Hz and 240V
      Apply Enhanced Droop Control → ω = ω_ref − M(e_P)(PID_f); V = V_ref −
  D(e_Q)(PID_V)
      Generate new references ω, V
      Send results to Synology via "droopoutput.php"
    Back on Synology NAS:
      "readdroopoutput.php" stores {timestamp, ω, V} in CSV format
    On the Simulink side:
      "ReadDroopOutputHTTP.m" reads the new references ω, V from Synology
      Update inverter reference signals
      Generate PWM signals → F28335 hardware
  Repeat loop
```

Fig. 5 presents the simplified Simulink model used for system validation, while Table 5 illustrates the corresponding parameter configurations. This model integrates photovoltaic generation, inverter, and load subsystems, all connected to the point of common coupling (PCC). The PCC block measures both active and reactive power, which is then transmitted via a communication interface to the Synology NAS, following the procedure outlined in the pseudocode. The NAS serves as an intermediary, hosting lightweight PHP scripts for data exchange with the ESP32 controller. The ESP32 executes the enhanced droop algorithm and returns optimized frequency and voltage references. These references are re-injected into the Simulink model to update the inverter control loop. This closed-loop interaction simulates the real-time behavior of a physical microgrid under the proposed control strategy.

4. Real-time experimental validation

This section presents the real-time validation results of the proposed edge–cloud coordinated control framework, tested under various real-world scenarios that include dynamic changes and faults within the microgrid system. The primary aim is to demonstrate that integrating an optimized droop control with PID-based virtual inertia emulation enhances microgrid stability in a cloud-coordinating environment. To evaluate microgrid performance under diverse dynamic conditions, four representative test scenarios, as specified in Table 6, are run using the setup illustrated in Fig. 6. These scenarios are selected to reflect typical microgrid disturbances, including load imbalances and faults. Each test is designed to challenge the controller's ability to regulate frequency and voltage within bounds specified in Table 4 and maintain fast transient response.

4.1. Results of disturbance scenarios

Fig. 7 illustrates the frequency and voltage responses of the microgrid under a 3-phase-to-ground fault initiated at t = 2.5 s (s), as indicated in Table 6 (S1). Compared to the conventional droop control with the proposed MOPSO-tuned droop strategy, the traditional droop controller exhibits pronounced oscillations in both frequency and

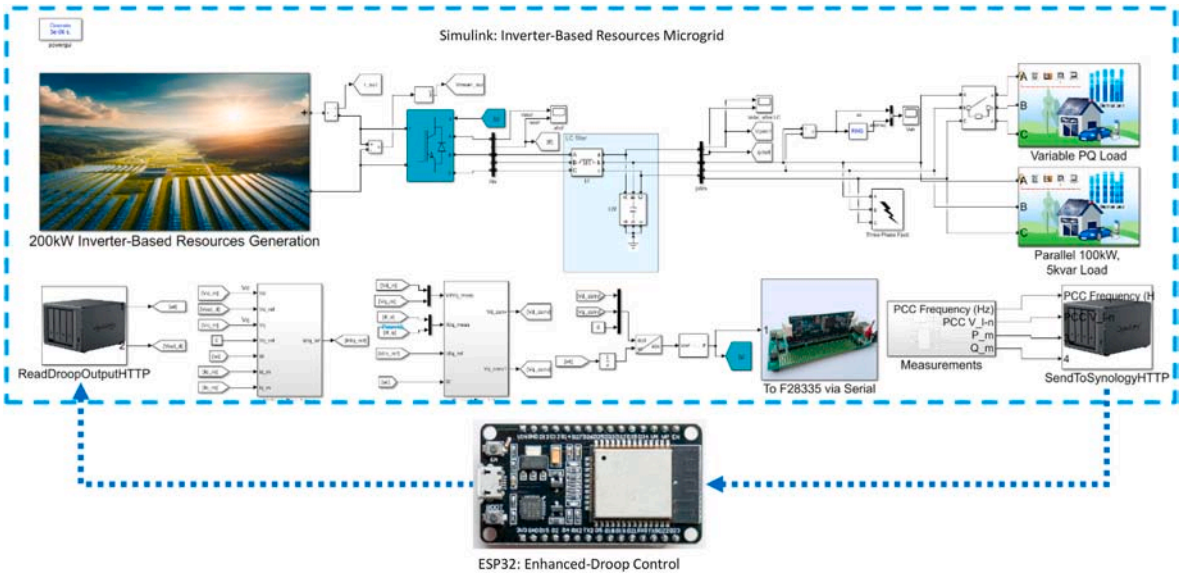

Fig. 5. Simplified Simulink schematic microgrid model with data exchange interface ESP32 and F28335.

voltage following the fault, reflecting poor damping and weak dynamic stability under high-disturbance conditions. In contrast, the MOPSO-tuned droop controller significantly enhances system resilience. Frequency deviations are notably suppressed, demonstrating improved damping behavior and convergence toward the nominal 50 Hz reference. The optimized droop control strategy reduced the post-fault voltage spick from approximately 700 V (V) to 330 V, a significant reduction of over 47%. The MOPSO-tuned controller does exhibit some residual oscillation in its frequency response; however, the deviations remain well within acceptable limits, even during a severe three-phase-to-ground fault. While the performance of the scheme does experience a slight decline during these severe faults, leading to a minor frequency overshoot, these short-term oscillations are expected during high-impact disturbances. Importantly, they do not compromise system stability, as the controller swiftly restores the frequency to its nominal value. Moreover, in practical microgrids, protection mechanisms would isolate any faulted sections if the disturbance persists for more than a few seconds, thereby preventing any long-term frequency excursions. This demonstrates the effectiveness of the proposed method in mitigating high voltage transients compared to the conventional control method. The reduction in both overshoot and settling time confirms the controller's ability to emulate inertia-like dynamics through optimal gain selection. This finding validates the effectiveness of the proposed strategy in mitigating the impact of severe symmetrical faults in low-inertia microgrid environments.

Table 5
Simulink model configuration parameters.

Parameter	Typical value	Description
Nominal frequency	50Hz	Rated grid frequency
Nominal voltage	240V	PCC RMS voltage
DC-link voltage	1000V	Input to the inverter
Sampling period	5e-6s	Control and measurement step
Droop gain (P–f)	5e-6	Frequency–power droop gain
Droop gain (Q–V)	3e-6	Voltage–reactive power droop gain
Communication refresh interval	1s	Simulink–NAS–ESP32 exchange cycle

Table 6
Experimental test scenarios.

Scenario	Description	Control focus
S1	Short-duration voltage sag (two and three-phase-to-ground fault)	Transient voltage support, droop responsiveness
S2	Sudden 75% load increase	Frequency dip recovery, inertial response
S3	Sudden 75% load decrease	Overshoot suppression, damping behaviour
S4	Step change in reactive load	Voltage regulation and steady-state voltage error

To further validate the response of the enhanced system under scenario S1, Fig. 8 illustrates the optimized low-inertia microgrid controller's reaction to multiple fault conditions, including single-phase, two-phase, and three-phase-to-ground faults occurring near the load side. Using the optimized edge-assisted control, the system achieved stable and acceptable voltage and frequency responses, indicating consistent and stable dynamic behavior across all fault scenarios. Compared to the previous study presented in Ref. [34], which relied on a PSO-tuned generalized droop control deployed on Arduino hardware, the current approach demonstrates substantial improvements in both control performance and practical implementation. The effectiveness of the proposed hybrid algorithm in both mitigating faults and adhering to performance demands makes it a viable solution for embedded deployment in edge computing, especially with advanced hardware such as Texas Instruments F28335 and ESP32. These outcomes validate the practical feasibility and robustness of the proposed real-time control strategy of low-inertia microgrids under varied fault conditions.

The effectiveness of the optimized edge-assisted control is further validated under sudden active and reactive load disturbances, as illustrated in Figs. 9 and 10. For instance, in Fig. 9, the microgrid underwent an abrupt injection and removal of a 75 kW active load at t = 0.9s, represented by the blue and red traces, respectively. The frequency response in Fig. 9 (a) shows remarkable resilience, with deviations contained within (±0.02 Hz). The disturbances are referred to as S2 and S3 in Table 6 to validate the internal response and overshoot suppression. This demonstrates that the optimized edge-assisted control in a cloud-coordinating environment effectively mitigates the inertia issue despite the absence of a physical rotating mass provided by the synchronous generator. In parallel, the voltage profile shown in Fig. 9(b) momentarily spiked before stabilizing within 200 ms. This transient suppression showcases the performance of the hybrid algorithm, as the optimized controller effectively adapts its gains in real-time to mimic the inertial properties of a traditional power system. The corresponding power trajectory in Fig. 9 (c) confirms the active load injection (+75 kW) and load shedding (−75 kW) events. The rapid return of active

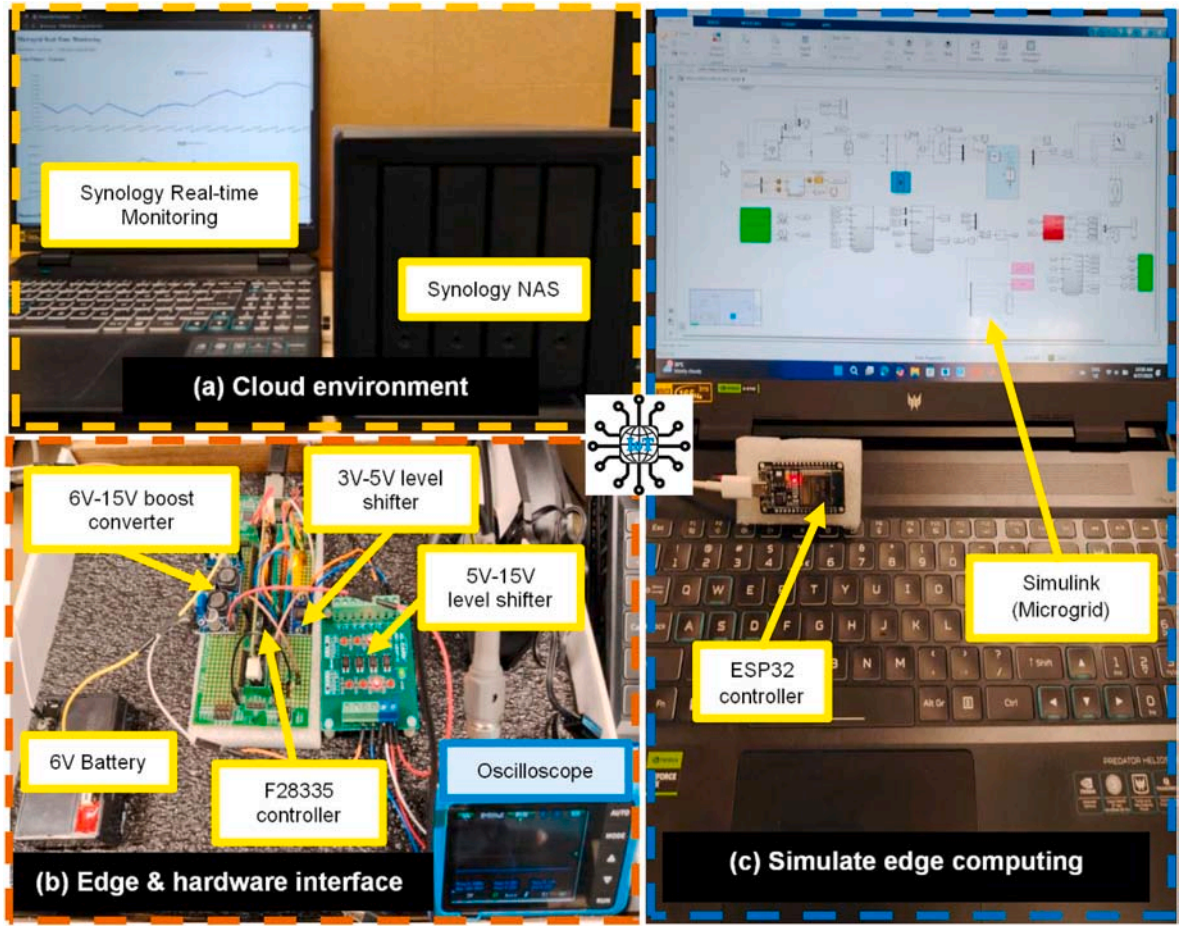

Fig. 6. An optimized edge-assisted CIL experimental setup: (a) cloud environment; (b) edge and hardware interface; (c) simulate edge computing.

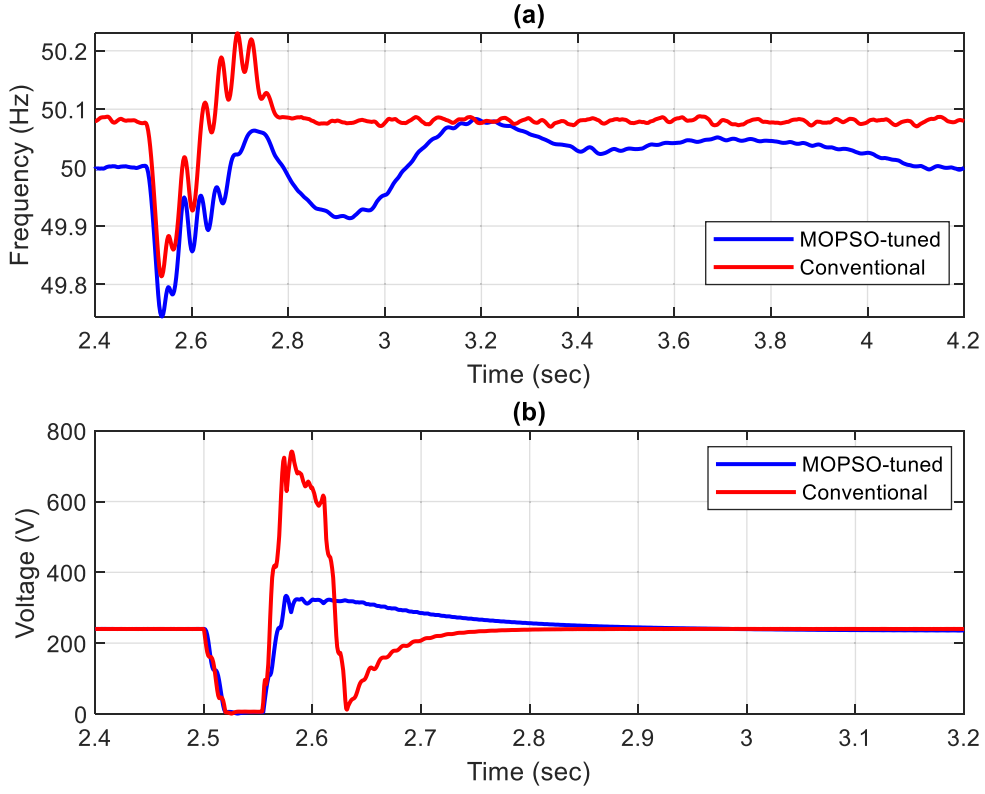

Fig. 7. 3-phase-to-ground fault; (a) frequency (b) voltage.

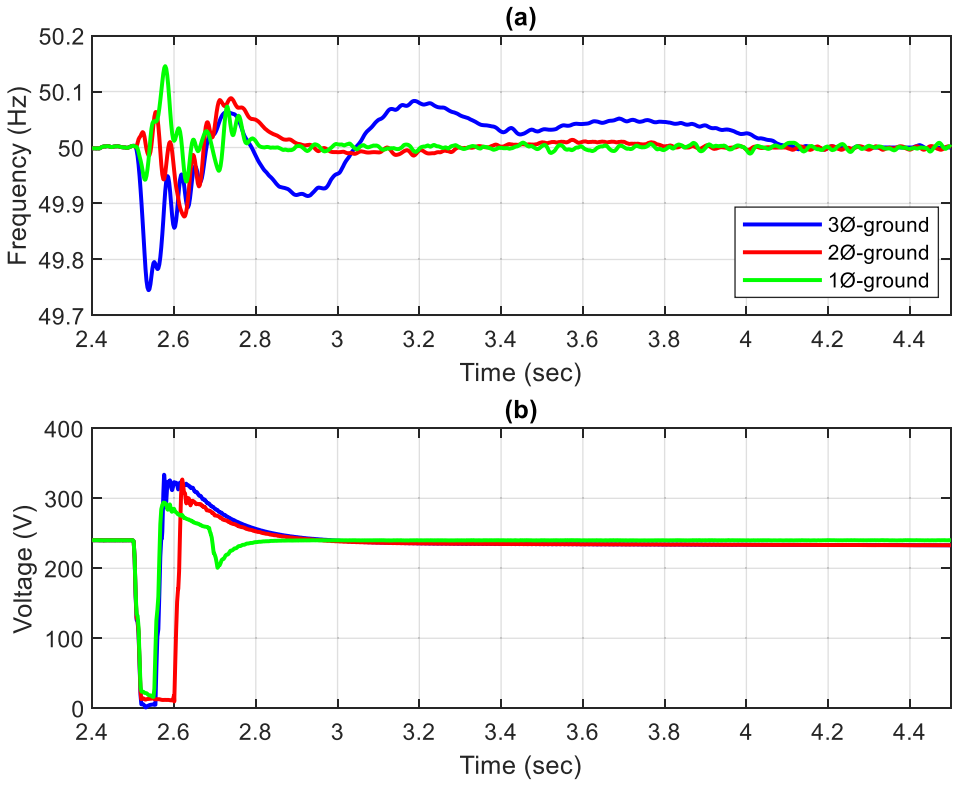

Fig. 8. System behavior during 1-3-phase-to-ground faults: (a) power frequency; (b) microgrid voltage.

power to baseline values without overshoot or oscillation further substantiates the real-time robustness of the edge-cloud executed control scheme. In islanded mode, the microgrid must maintain its own stability using only its local, low-inertia resources (e.g., inverters from renewable sources). The lack of a large inertial mass means that any significant load change leads to rapid and substantial fluctuations in voltage and frequency, highlighting a system weakness.

To accurately emulate fluctuating demand, system evaluation must account for both active and reactive power variations. In this regard, Fig. 10 shows the fast system response in managing dynamic changes

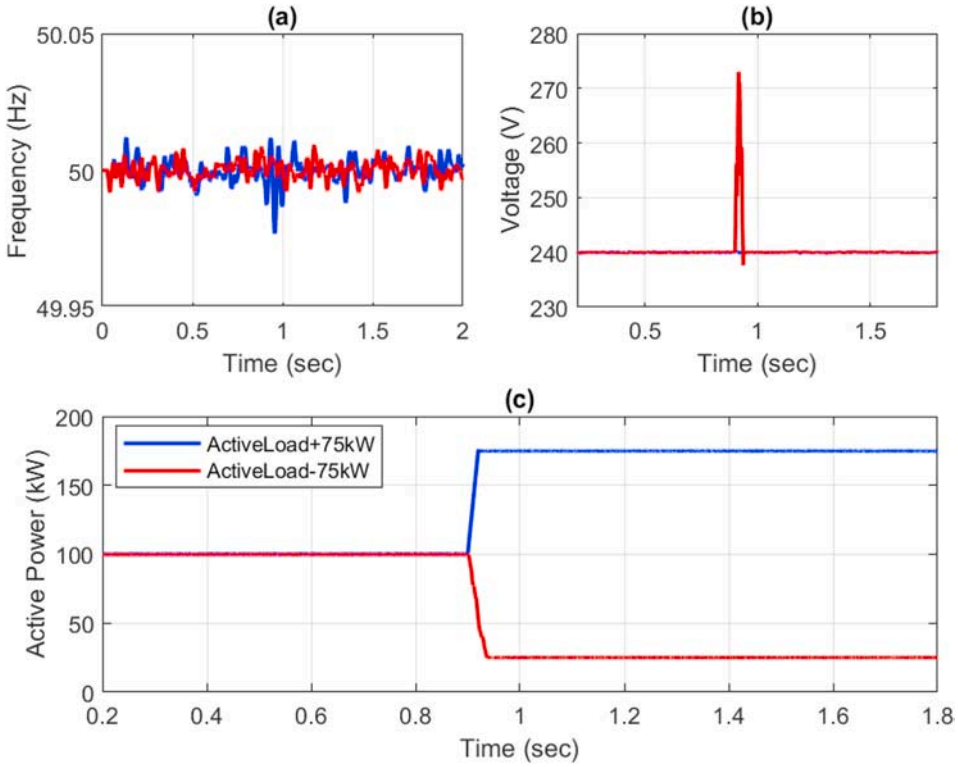

Fig. 9. Load disturbance: (a) frequency; (b) voltage; (c) active power.

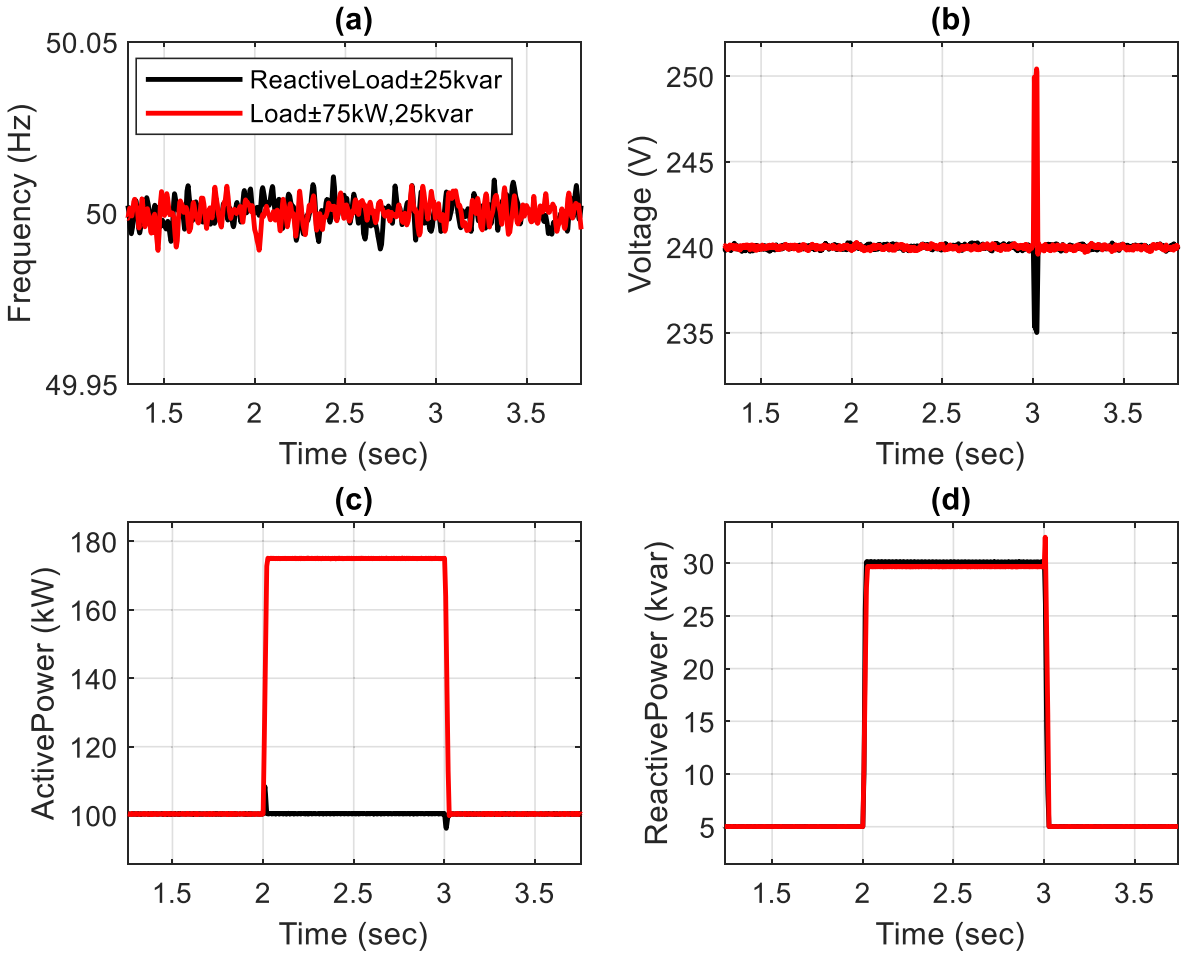

Fig. 10. Load disturbance: (a) frequency; (b) voltage; (c) active power; (d) reactive power.

under combined active and reactive disturbances. The reactive power step of 25 kVAR at t = 2s has been simulated, along with the same 75 kW active power disturbance, forming a dual-mode disturbance scenario as a combination of S2, S3, and S4. As seen in Fig. 10 (a), the frequency remains tightly regulated, maintaining operation within ±0.015 Hz of the nominal value. This reconfirms the success of virtual inertia control in a cloud-coordinating environment, even in the presence of multiple simultaneous perturbations. Experiencing a dip, the voltage response in Fig. 10 (b) recovered to the nominal 240 V in less than 150 ms, demonstrating a faster and more efficient performance than traditional droop control. Fig. 10 (c) and (d) illustrate the injected power profiles for active and reactive components, respectively. The clean transitions in both power types, with no persistent deviations, highlight the high responsiveness and stability provided by the optimized edge-assisted control. Overall, these experimental results verify that the proposed method effectively stabilizes voltage and frequency during significant step changes in both active and reactive loads. The emulation of virtual inertia through MOPSO-tuned droop control, implemented on a real-time ESP32 edge platform and the F28335 microcontroller, enables fast and accurate recovery actions. Unlike traditional droop control, which often experiences delayed responses and instability under low inertia conditions, this hybrid algorithm, integrated into an optimized cloud-based framework, offers enhanced disturbance rejection capabilities. This makes it particularly suitable for microgrids with high levels of renewable energy integration.

The objective of this study is to demonstrate the robustness and stability of the proposed approach in maintaining critical system parameters, specifically frequency and voltage, under various operating conditions. Fig. 11 illustrates the comparison of frequency and voltage performance during load disturbances before and after the implementation of the proposed control strategy. The results indicate that the technique effectively keeps frequency and voltage deviations within the typical acceptable limits for normal operations, meeting the required standards of ±0.1% to ±0.2%. This outcome reflects the method's ability to ensure system stability and reliability, particularly under low inertia conditions.

The simulation was performed using MATLAB/Simulink on a standard workstation rather than a dedicated real-time simulator. The closed-loop control cycle, which includes Simulink computation, HTTP transmission, ESP32 processing, and feedback updates, was measured to have a latency of approximately 1 s per cycle. This latency is significantly lower than the 1.5-s threshold commonly observed in similar cloud-integrated systems. Importantly, this level of latency does not impact system performance as seen in Fig. 12, particularly in frequency control, where rapid response is essential. Therefore, the platform operates effectively as a real-time CIL environment, making it suitable for validating the dynamic response behavior within the frequency control bandwidth of microgrid systems.

A review of prior studies indicates that while numerous works [32], [44], [45], [46] have achieved satisfactory frequency or voltage regulation during load variations, most have not accounted for fault scenarios. The current work addresses both load changes and fault conditions, demonstrating improved settling times. These findings do not assert superiority but rather extend existing research by highlighting the viability of implementing optimized droop-based controllers on real-time edge platforms. Building on prior studies, Fig. 13 displays the actual settling time observed during load variations, and Fig. 14 illustrates the settling time during various fault scenarios. Fig. 13 clearly

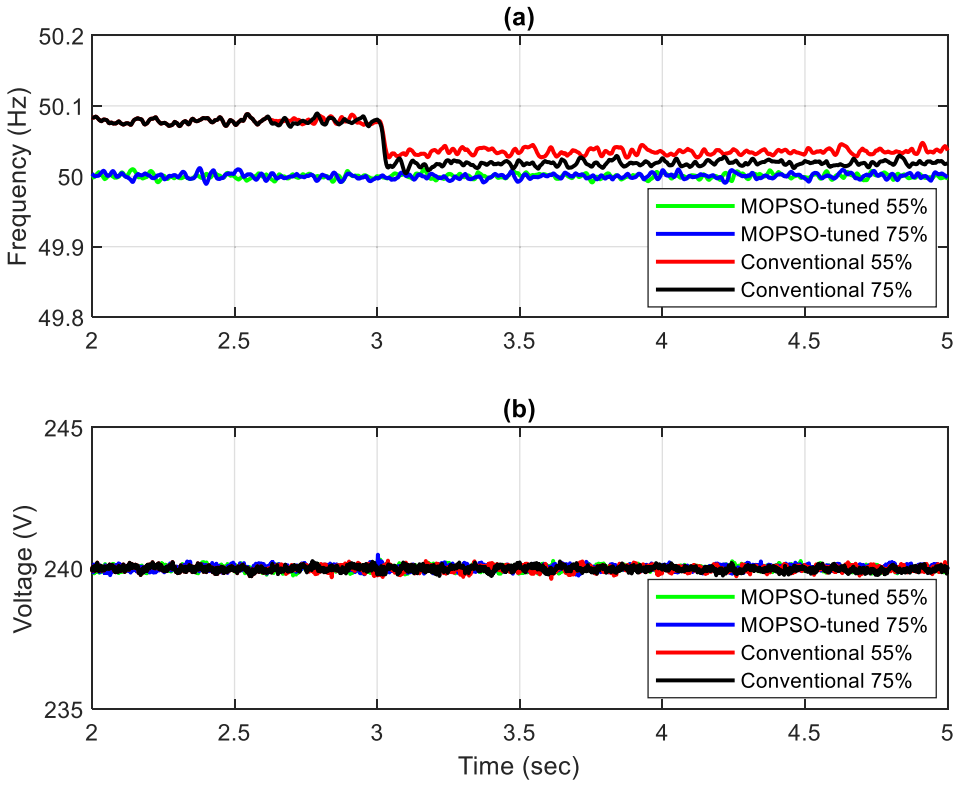

Fig. 11. Conventional and MOPSO-tuned droop control performance under varied load disturbances.

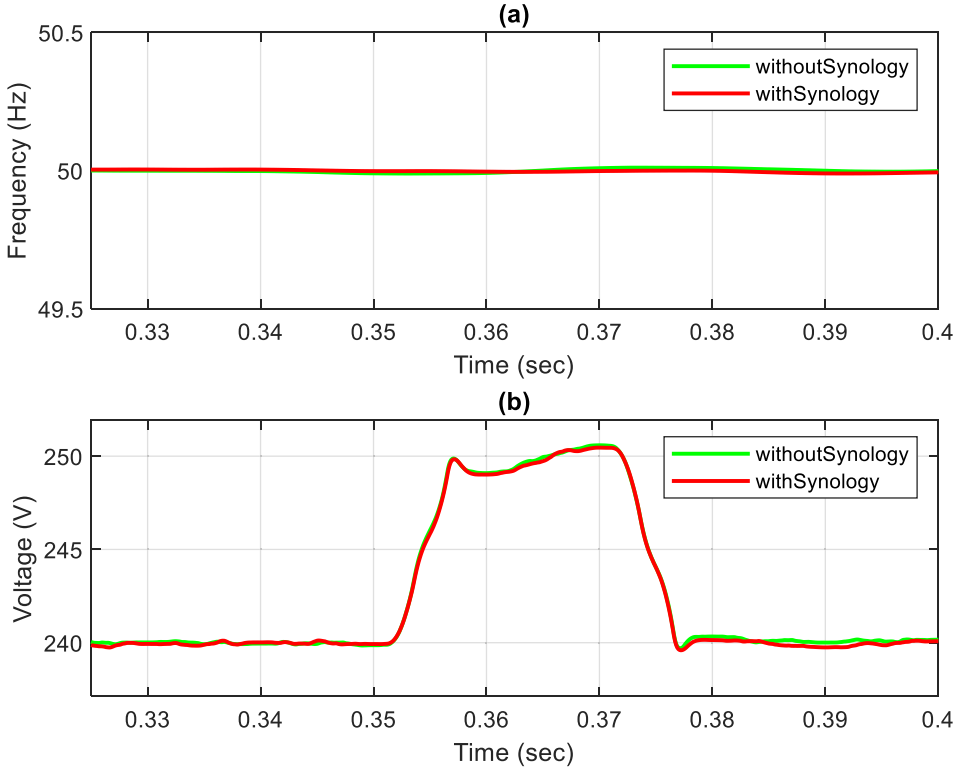

Fig. 12. System's timing performance with and without communication layers.

illustrates the performance comparison between the proposed method and other recent approaches. The optimized edge-assisted control, which is presented in the current work, consistently achieves the best performance. Specifically, it demonstrates a settling time of 0.1 s during load variation. This settling time is observed to increase in fault scenarios, a result attributed to the greater severity of the fault conditions.

In the experimental setup, the optimization process is carried out offline rather than within the real-time loop. Specifically, the MOPSO

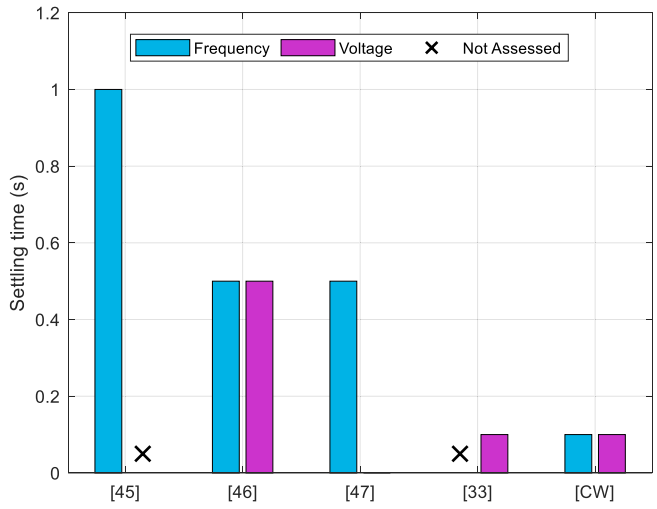

Fig. 13. Settling time during load variation.

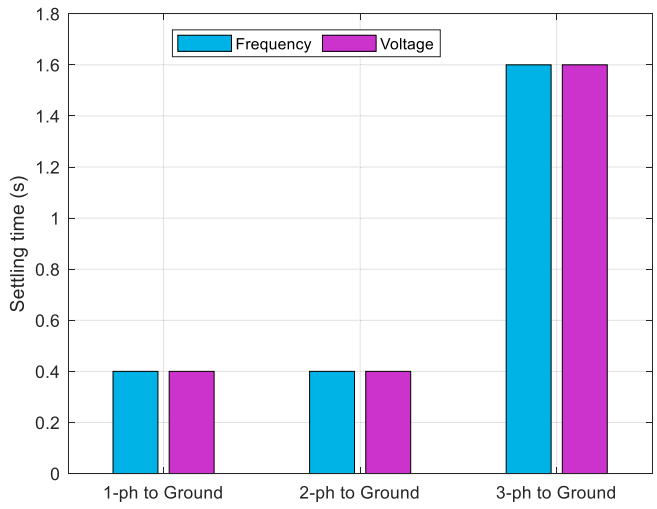

Fig. 14. Settling time during fault scenarios.

executes offline, and the tuned PID parameters are then deployed to the ESP32 controller. The closed-loop operation involves continuous interaction among the Simulink microgrid model, the Synology NAS, and the ESP32, demonstrating a CIL environment. This study utilizes the Simulink Desktop Real-Time (SLDRT) kernel, which offers a real-time execution layer on the host machine. The ESP32 controller operates in a closed loop with the simulated microgrid system through continuous data exchange with bounded timing. The execution cycle of approximately 1 s aligns with the real-time operational bandwidth required for primary and secondary microgrid control. While the dedicated real-time simulators like OPAL-RT or Speedgoat are not employed, the developed platform in this study meets the criteria for CIL testing for embedded controller verification, where a physical controller interacts directly with a real-time simulation kernel. Throughout the entire testing of dynamic scenarios, the Simulink modelled microgrid remains continuously interfaced with the ESP32-based edge controller via HTTP communication, facilitated through the Synology NAS platform. In the closed-loop framework, Simulink performs control computations and state observations while also generating the PWM signals needed to drive the inverter. To ensure the physical operation of the inverter, the PWM signals generated in Simulink are routed to a Texas Instruments F28335 controller, as shown in Fig. 15 (a). This controller acts as the hardware PWM generator and serves as an interface between the digital control model and the hardware layer, effectively driving the inverter. A level-shifting circuit is used because the F28335 controller outputs signals at a 3.3V logic level. This voltage is inadequate for the gate driver circuits, which require input voltages between 15V and 24V to function properly with the actual inverter hardware, as shown in Fig. 15(b). The level shifter acts as an intermediary, converting the 3.3V control signal into a 24V signal. This conversion ensures proper communication and compatibility between the low-voltage controller and the high-voltage gate drivers, as depicted in Fig. 15 (c). The entire process flows from edge-cloud control execution on the ESP32 to PWM waveform generation in the microgrid Simulink model, culminating in the final operation of the physical inverter via the F28335 and level-shifted signals. This setup validates the operation of the CIL microgrid control system within a cloud coordinating environment.

Figs. 16–18 illustrate the Synology Real-Time Monitoring System. They show the simulation time step and the observation window used for system evaluation. The use of short, overlapping windows allows for the capture of rapid transients without interference from surrounding steady-state data. Fig. 16 illustrates data during a two-phase-to-ground fault at 30 s, and during a three-phase-to-ground fault, as shown in Fig. 17. Fig. 18 displays the Synology monitoring data during load injection (75 kW, 5 kvar) at 2 s and load removal (75 kW, 5 kvar) at 3 s. All figures pertain to droop output setpoints from the ESP32 and measured data from the Simulink Microgrid, focusing on frequency, voltage, active power, and reactive power. These figures validate the Synology real-time monitoring system through CIL experiments. They showcase live, closed-loop data exchange between Simulink (the plant), Synology, and the ESP32 (the controller). During each cycle, the ESP32 calculates the angular frequency and voltage setpoints, which are then sent back through Synology for the subsequent update. The data stored on the Synology NAS can be easily exported in Excel format, as it is saved in CSV format. Referring to Figs. 16–18, frequency and voltage tracking are successfully achieved from various initial frequency and voltage points. It is important to note that relying solely on frequency or voltage error can lead to a slow system response. This approach may cause lag or oscillation because the controller can only adjust based on the current error, without anticipating future changes in frequency or voltage. The optimized edge-assisted control for low-inertia microgrids is designed to continuously predict and adjust control parameters in real-time, based on the duration and rate of change of any deviations. It actively monitors and anticipates grid fluctuations, ensuring that frequency and voltage deviations are minimized, ideally approaching zero.

4.2. Key takeaways of discussion

Prior work [30] has implemented a PSO-tuned Generalized Droop Controller (GDC) on an Arduino Mega 2560. The setup involved collecting real-time power measurements and transmitting this data serially to a microcontroller, which then sends it to ThingSpeak for cloud-based storage, real-time visualization, reference data processing, and updating. Although the system demonstrated functional control, it suffered from significant delays (~15 s) due to ThingSpeak's data update interval. Moreover, the complexity of the GDC algorithm exceeded Arduino's real-time processing capability, limiting its effectiveness as a lightweight embedded edge platform. This study addresses existing limitations by directly embedding the MOPSO-tuned controller into the ESP32. This approach enables true real-time operation (with a response time of approximately 1 s), scalable deployment, and robust performance through an edge–cloud coordination framework. The primary findings validate the effectiveness of the control strategy in managing low-inertia microgrids within a cloud-based environment. Utilizing a hybrid algorithm (see Fig. 1) that incorporates an edge-assisted approach and optimization achieves high resilience against both stable operating conditions and unexpected disturbances. The confirmed effectiveness of the optimized control strategy, as supported by the results obtained across key performance metrics, suggests it offers a viable solution for managing microgrids through smart coordination between

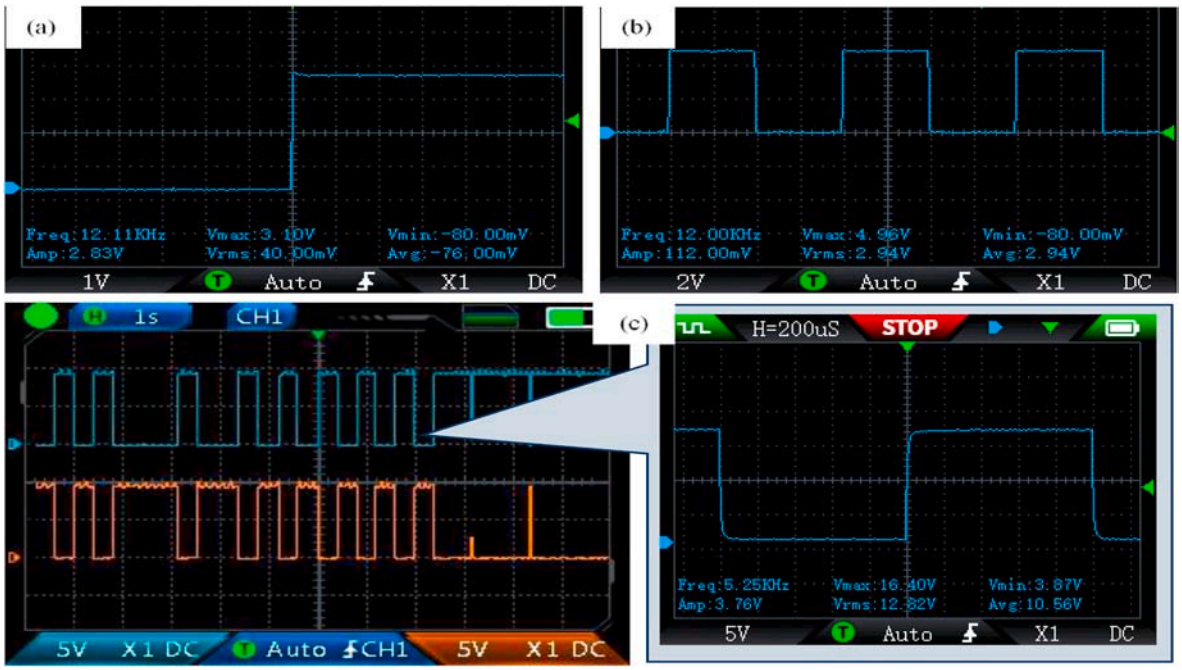

Fig. 15. Measured PWM signal; (a) level shifter 3V; (b) after level shifter 5V; (c) Boosted to a 15V PWM signal (inverting and non-inverting) for one phase inverter switching.

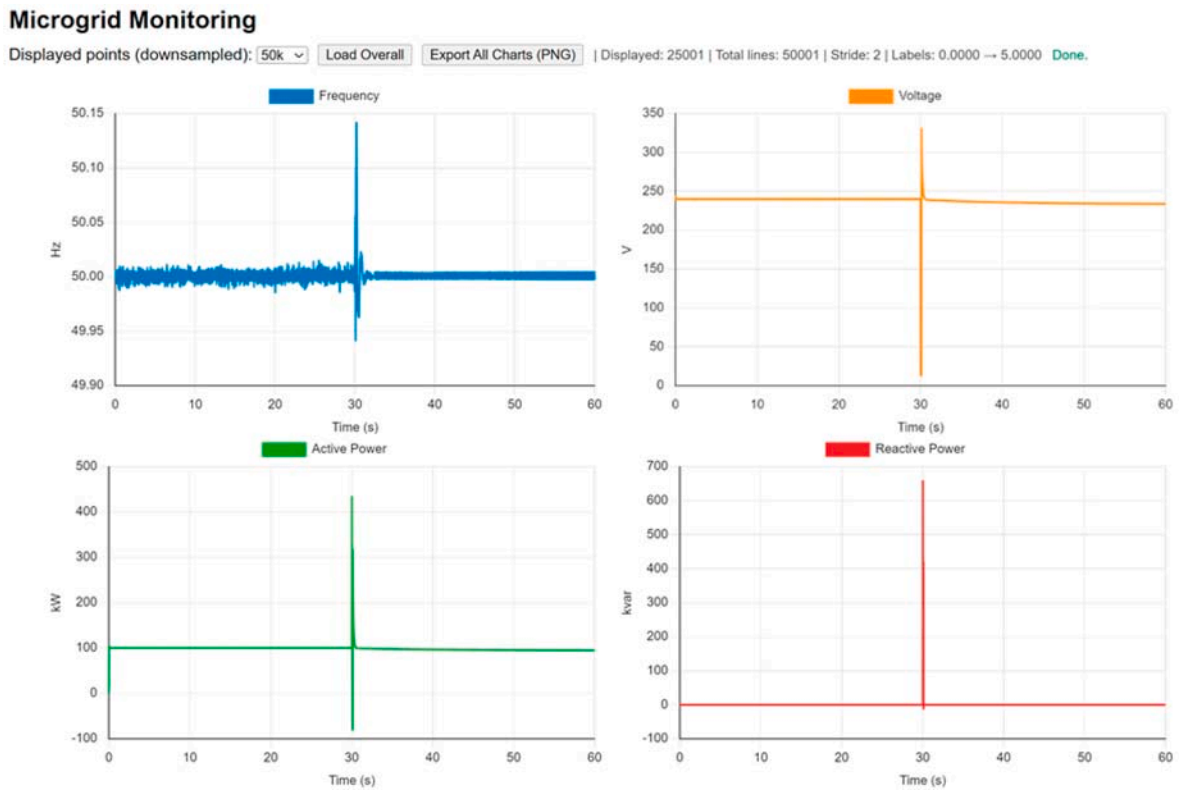

Fig. 16. Synology monitoring data during both steady-state and two-phase-to-ground fault conditions.

edge devices and the cloud. The intelligent tuning of both droop and control gains allows the system to provide fast frequency and voltage recovery, thereby emulating the stabilizing effects of physical inertia. Moreover, the MOPSO-tuned droop control approach is simpler, computationally lighter, and readily implementable in edge devices like the ESP32 and F28335 controllers, making it highly suitable for real-time microgrid applications. The successful testing of the hybrid algorithm shown in Fig. 1 confirms that its real-time performance on embedded hardware aligns with the predictive performance from its Simulink model, validating the reliability of the hardware implementation. The key performance indicators that demonstrate the effectiveness of the proposed strategy are detailed as follows:

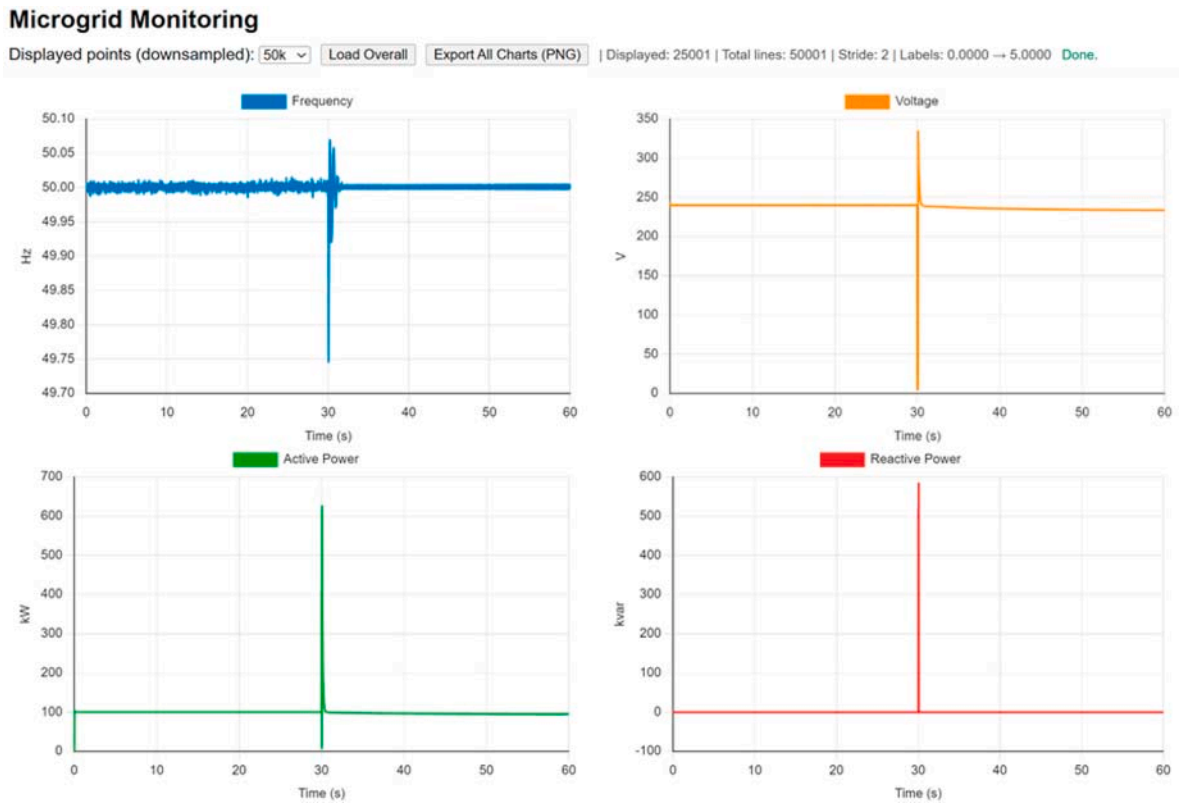

Fig. 17. Synology monitoring data during both steady-state and three-phase-to-ground fault conditions.

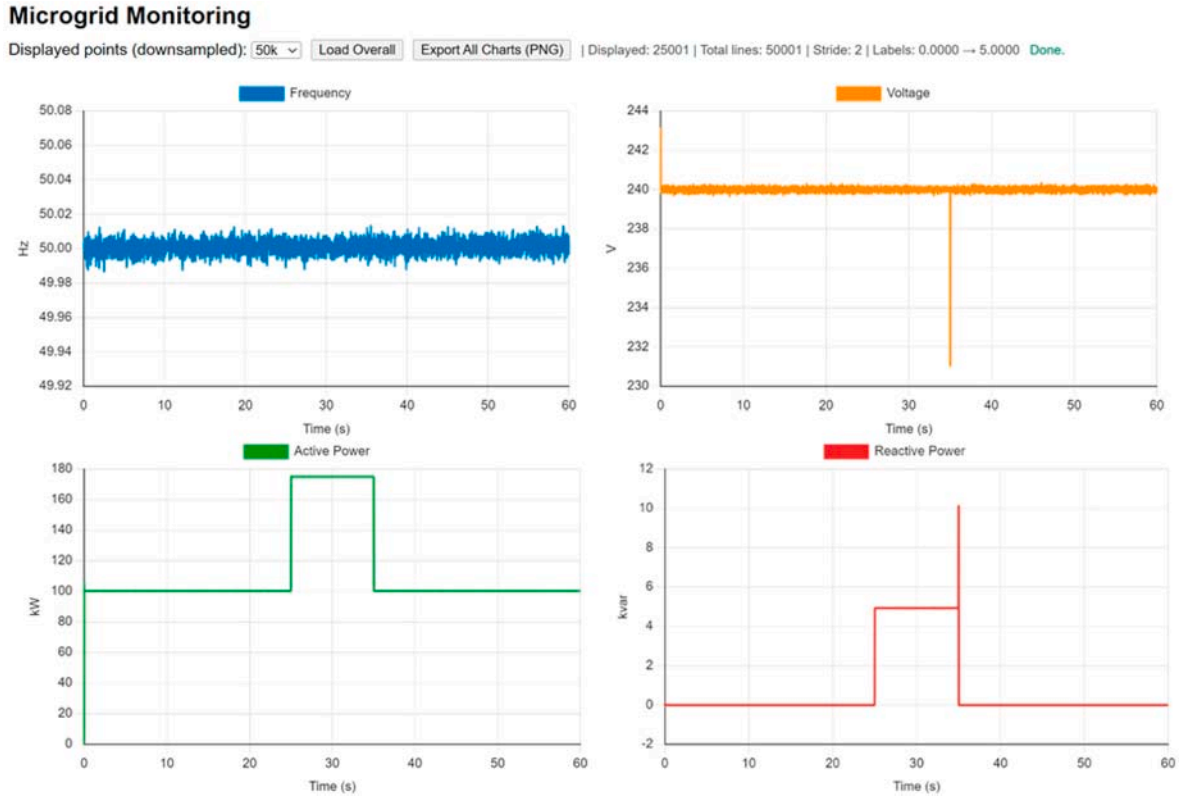

Fig. 18. Synology monitoring data during both load injection and load removal conditions.

- *Frequency Stability:* Under varying load conditions and fault disturbances, the frequency deviation remains within ±5% of the nominal 50 Hz reference. This reflects strong dynamic stability and improved damping, attributed to the dual PID and the droop gain optimization.

- *Voltage Regulation:* The system maintains voltage deviations within ±5% of the 240 V nominal, even under severe transient events such as a 3-phase-to-ground fault, where voltage spikes are reduced by more than 47% compared to the conventional droop controller.
- *Scalability and Reliability:* The results presented in the previous section demonstrate that the system performs effectively under various fault scenarios, including single-phase, two-phase, and three-phase faults near the load terminal. The consistent recovery and tracking behavior observed in all test conditions validate the reliability and practicality of implementing the control system in real-world applications.

Although the proposed framework demonstrates effective closed-loop stabilization in a controller-in-the-loop environment, several practical limitations remain before deployment in real electric systems. First, the current architecture relies on communication quality among Simulink, the Synology NAS, and the ESP32 controller. Variations in latency, packet loss, server refresh cycles, or network congestion may influence timing consistency and control responsiveness. Second, the present implementation relies on lightweight HTTP-based exchange, which is suitable for feasibility validation but does not yet provide full interoperability with industrial communication standards typically used in practical smart-grid environments. Third, the current study does not assess communication failures, cyber-physical attacks, or multi-device interoperability under heterogeneous field protocols. Therefore, the proposed system should be viewed as a cost-effective proof-of-concept for edge-cloud-coordinated microgrid control. Future work should investigate protocol-standardized interoperability, time-synchronized communication, cybersecurity hardening, and deployment on dedicated real-time or field-level platforms.

5. Conclusion

This paper presents a real-time implementation of an optimized edge–cloud coordinated control system for low-inertia microgrids, featuring the MOPSO-tuned droop control strategy with dual PID loops. Unlike classical droop systems or model-based virtual inertia controllers, the proposed method utilizes MOPSO to enhance frequency and voltage stability without relying on differential swing dynamics. The controller's structure remains computationally lightweight, yet it emulates inertia-like behavior through optimized gain selection. The design integrates a Simulink-modelled microgrid with an ESP32-based embedded controller via a Synology NAS, forming a scalable and low-latency edge–cloud control loop. The PWM waveforms generated by the Simulink model are executed on the F28335 microcontroller to control the microgrid inverters. The CIL experiments validate the controller's ability to maintain frequency and voltage during load variations and multiple fault scenarios, including three-phase-to-ground faults. Compared to conventional droop and previous PSO-based implementations, the proposed system significantly reduces overshoot, accelerates system recovery, and achieves real-time control performance suitable for field deployment. The proposed work offers a significant practical contribution by demonstrating the feasibility of executing MOPS-based droop control on the low-cost ESP32 microcontroller, a platform typically used for general IoT applications. This showcases a cost-effective solution for decentralized microgrid control. The TI-F28335 digital signal processor, known for its high-performance floating-point unit and real-time processing capabilities, serves as a high-fidelity platform for validating the ESP32 implementation. Future research should focus on utilizing cloud computing and machine learning to improve inertia emulation and energy management in hybrid microgrids. This approach will leverage high-performance computation and data processing capabilities essential for real-time optimization, predictive analytics, and adaptive control strategies. Additionally, more sophisticated CIL experiments can be conducted using industry-standard platforms such as OPAL-RT, Speedgoat, or RTDS, assuming these specialized facilities are available.

CRediT authorship contribution statement

Yiizzan Suffian: Writing – original draft, Validation, Software, Methodology, Formal analysis, Data curation. **Ahmed M.A. Haidar:** Writing – review & editing, Supervision, Methodology, Investigation, Funding acquisition, Conceptualization. **Tony Ahfock:** Writing – review & editing, Visualization.

Declaration of competing interest

The authors declare that they have no known competing financial interests or personal relationships that could have appeared to influence the work reported in this paper.

Acknowledgements

The authors gratefully acknowledge the support from the Ministry of Higher Education (Malaysia) under the Fundamental Research Grant Scheme (FRGS/1/2021/TK0/UNIMAS/02/3).

Data availability

Data will be made available on request.

References

[1] Agboola Benjamin Alao, Olatunji Matthew Adeyanju, Manohar Chamana, Stephen Bayne, Argenis Bilbao, Optimized universal droop control framework for enhancing stability and resilience in renewable-dense power grids, Electronics 14 (11) (2025) 2149, https://doi.org/10.3390/electronics14112149.
[2] Muhammad Qasim Khan, Mohamud Ahmed Musse, Ahmed M.A. Haidar, An accurate algorithm of PMU-based wide area measurements for fault detection using positive-sequence voltage and unwrapped dynamic angles, Measurement 192 (2022) 110906, https://doi.org/10.1016/j.measurement.2022.110906.
[3] T.K. Roy, A.M. Than Oo, Enhancing grid frequency regulation in low inertia modern multi-area power systems using cascaded non-integer control approaches with BESS-based virtual inertia, IET Renew. Power Gener. 18 (2024) 4602–4620, https://doi.org/10.1049/rpg2.13169.
[4] M.A. Hasan, M.S. Hossain, M.A. Roslan, A. Azmi, L.J. Hwai, A.A. Nazib, N. S. Ahmad, Optimized droop control strategy for efficiency improvement in islanded AC microgrid, IFAC J. Syst. Control 33 (2025), https://doi.org/10.1016/j.ifacsc.2025.100319.
[5] I. Ray, L.M. Tolbert, Grid-forming inverter control design for PV sources considering DC-link dynamics, IET Renew. Power Gener. 19 (1) (Jan. 2025), https://doi.org/10.1049/rpg2.12454.
[6] B. Alghamdi, Fuzzy logic–based decentralized voltage–frequency control and inertia control of a VSG-Based isolated microgrid system, Energies 15 (22) (Nov. 2022) 8401, https://doi.org/10.3390/en15228401.
[7] C. Zhou, Y. Liao, K. Zhang, X. Xu, J. Liao, Virtual inertia based hierarchical control scheme for distributed generations considering communication delay, Front. Energy Res. 11 (2023), https://doi.org/10.3389/fenrg.2023.1135038.
[8] D.B. Rathnayake, et al., Grid forming inverter modeling, control, and applications, IEEE Access 9 (2021) 114781–114807, https://doi.org/10.1109/ACCESS.2021.3104617.
[9] K.Y. Yap, C.R. Sarimuthu, J.M.Y. Lim, Virtual Inertia-based Inverters for Mitigating Frequency Instability in grid-connected Renewable Energy System: a Review, MDPI AG, Dec. 01, 2019, https://doi.org/10.3390/app9245300.
[10] H.M. Hussein, S.M.S.H. Rafin, M.S. Abdelrahman, O.A. Mohammed, Hardware implementation of a resilient energy management system for networked microgrids, World Electr. Vehic. J. 15 (5) (May 2024), https://doi.org/10.3390/wevj15050209.
[11] B. Muftau, M. Fazeli, The role of virtual synchronous machines in future power systems: a review and future trends. Electric Power Systems Research, Elsevier Ltd., May 01, 2022, https://doi.org/10.1016/j.epsr.2022.107775.
[12] M. Talaat, A.S. Alsayyari, A. Alblawi, A.Y. Hatata, Hybrid-cloud-based data processing for power system monitoring in smart grids, Sustain. Cities Soc. 55 (Apr. 2020) 102049, https://doi.org/10.1016/J.SCS.2020.102049.
[13] J. Li, C. Gu, Y. Xiang, F. Li, Edge-cloud computing systems for smart grid: state-of-the-art, Architecture, and applications, J. Mod. Power Syst. Clean Energy 10 (4) (Jul. 2022) 805–817, https://doi.org/10.35833/MPCE.2021.000161.
[14] Yousef Asadi, Mohsen Eskandari, Milad Mansouri, "Integration of DRL-driven edge computing for adaptive synthetic inertia allocation in grid-forming BESSs under spatial frequency variations, J. Energy Storage 141 (Part B) (2026) 119065, https://doi.org/10.1016/j.est.2025.119065.

[15] R. Rosso, X. Wang, M. Liserre, X. Lu, S. Engelken, Grid-Forming Converters: Control Approaches, Grid-Synchronization, and Future Trends - a Review, Institute of Electrical and Electronics Engineers Inc, 2021, https://doi.org/10.1109/OJIA.2021.3074028.
[16] M. Zelba, et al., A grid-tied inverter with renewable energy source integration in an off-grid system with a functional experimental prototype, Sustainability 14 (20) (Oct. 2022), https://doi.org/10.3390/su142013110.
[17] H. Bevrani, Q. Shafiee, H. Golpîra, "Frequency Stability and Control in Smart Grids - IEEE Smart Grid." [Online]. Available: https://smartgrid.ieee.org/bulletins/september-2019/frequency-stability-and-control-in-smart-grids. (Accessed 28 February 2025).
[18] A.M. Jasim, B.H. Jasim, V. Bureš, P. Mikulecký, A new decentralized robust secondary control for smart islanded microgrids, Sensors 22 (22) (Nov. 2022) 8709, https://doi.org/10.3390/s22228709.
[19] V.N. Ogar, S. Hussain, A. Gamage, Load frequency control using the particle swarm optimisation algorithm and PID controller for effective monitoring of transmission line, Energies 16 (15) (Aug. 2023), https://doi.org/10.3390/en16155748, 5748–5748.
[20] M. Lotfi, G.J. Osório, M.S. Javadi, M.S. El Moursi, C. Monteiro, J.P.S. Catalão, A fully decentralized machine learning algorithm for optimal power flow with cooperative information exchange, Int. J. Electr. Power Energy Syst. 139 (Jul) (2022), https://doi.org/10.1016/j.ijepes.2022.107990.
[21] K. El Mezdi, A. El Magri, L. Bahatti, Advanced control and energy management algorithm for a multi-source microgrid incorporating renewable energy and electric vehicle integration, Results Eng. 23 (Sep) (2024), https://doi.org/10.1016/j.rineng.2024.102642.
[22] Y. Kabalci, E. Kabalci, S. Padmanaban, J.B. Holm-Nielsen, F. Blaabjerg, Internet of Things Applications as Energy Internet in Smart Grids and Smart Environments, MDPI AG, Sep. 01, 2019, https://doi.org/10.3390/electronics8090972.
[23] Z. Guan, J. Li, L. Wu, Y. Zhang, J. Wu, X. Du, Achieving efficient and secure data acquisition for cloud-supported internet of things in smart grid, IEEE Internet Things J. 4 (6) (Dec. 2017) 1934–1944, https://doi.org/10.1109/JIOT.2017.2690522.
[24] J.C.M. Siluk, P.S. de Carvalho, V. Thomasi, C.A. de O. Pappis, J.L. Schaefer, Cloud-based energy management systems: terminologies, concepts and definitions, Energy Res. Social Sci. 106 (2023) 103313, https://doi.org/10.1016/j.erss.2023.103313. ISSN 2214-6296.
[25] Chongxin Huang, Song Deng, Hui Ge, Resilient load frequency control of cyber–physical power systems with off-the-shelf redundant communication channels under FDI attacks, Measurement: Energy 7 (2025) 100053, https://doi.org/10.1016/j.meaene.2025.100053.
[26] Dayu Wang, Daojun Zhong, Alireza Souri, Energy management solutions in the internet of things applications: technical analysis and new research directions, Cogn. Syst. Res. 67 (2021) 33–49, https://doi.org/10.1016/j.cogsys.2020.12.009. ISSN 1389-0417.
[27] Y.Y. Chen, Y.H. Lin, A smart autonomous time-and frequency-domain analysis current sensor-based power meter prototype developed over fog-cloud analytics for demand-side management, Sensors (Switzerland) 19 (20) (Oct. 2019), https://doi.org/10.3390/s19204443.
[28] M.B.R. Xu, Managing renewable energy and carbon footprint in multi-cloud computing environments, J. Parallel Distr. Comput. 135 (Jan. 2020) 191–202.
[29] T. Pu, et al., Power flow adjustment for smart microgrid based on edge computing and multi-agent deep reinforcement learning, J. Cloud Comput. 10 (1) (Dec. 2021), https://doi.org/10.1186/s13677-021-00259-1.
[30] S.A. Hashmi, C.F. Ali, S. Zafar, Internet of things and cloud computing-based energy management system for demand side management in smart grid, Int. J. Energy Res. 45 (1) (Jan. 2021) 1007–1022, https://doi.org/10.1002/er.6141.
[31] D. Wang, F. Zhou, J. Li, Cloud-based parallel power flow calculation using resilient distributed datasets and directed acyclic graph, J. Mod. Power Syst. Clean Energy 7 (1) (January 2019) 65–77, https://doi.org/10.1007/s40565-018-0406-4.
[32] H. Zhao, Y. Zhu, K. Lu, Q. Li, Z. Li, S. Dong, Edge computing and hybrid control technology for microgrids based on activity on edge networks, Energy Convers. Econ. 4 (6) (Dec. 2023) 387–400, https://doi.org/10.1049/enc2.12103.
[33] J. Liu, Y. Ma, Y. Chen, C. Zhao, X. Meng, J. Wu, Multi-agent deep reinforcement learning-based cooperative energy management for regional integrated energy system incorporating active demand-side management, Energy 319 (Mar) (2025), https://doi.org/10.1016/j.energy.2025.135056.
[34] Y. Suffian, A.M.A. Haidar, W.A. Abidin, H.M. Basri, An improved hybrid method combined with a cloud-based supervisory control to facilitate smooth coordination under low-inertia grids, Progress Eng. Sci. 2 (2) (Jun. 2025), https://doi.org/10.1016/j.pes.2025.100072.
[35] Z. Majd, M. Kalantar, A novel cost-effective voltage fluctuations management in a droop-controlled islanded microgrid, IET Renew. Power Gener. 17 (2) (Feb. 2023) 317–335, https://doi.org/10.1049/rpg2.12599.
[36] K.N. Yogithanjali Saimadhuri, M. Janaki, Advanced control strategies for microgrids: a review of droop control and virtual impedance techniques, Results Eng. 25 (2025) 103799, https://doi.org/10.1016/j.rineng.2024.103799. ISSN 2590-1230.
[37] Usman Bashir Tayab, Mohd Azrik Bin Roslan, Leong Jenn Hwai, Muhammad Kashif, A review of droop control techniques for microgrid, Renew. Sustain. Energy Rev. 76 (2017) 717–727, https://doi.org/10.1016/j.rser.2017.03.028. ISSN 1364-0321.
[38] Tu, B., Xu, X., Gu, Y., Deng, K., Xu, Y., Zhang, T., Gao X., Wang, K., & Wei, Q. Improved droop control strategy for islanded microgrids based on the adaptive weight particle swarm optimization algorithm. Electronics, 14(5), 893. https://doi.org/10.3390/electronics14050893.
[39] Vijayakumar Gali, Prashant Kumar Jamwal, Nitin Gupta, B. Chitti Babu, Ajay Kumar, An auto-tuned droop coefficient-based controller for microgrid system to enhance grid resilience during blackouts, Sustain. Energy Technol. Assessments 57 (2023) 103313, https://doi.org/10.1016/j.seta.2023.103313.
[40] J. Yao, X. Luo, F. Li, et al., Research on hybrid strategy particle swarm optimization algorithm and its applications, Sci. Rep. 14 (2024) 24928, https://doi.org/10.1038/s41598-024-76010-y.
[41] Q. Hong, et al., A new load shedding scheme with consideration of distributed energy resources' active power ramping capability, IEEE Trans. Power Syst. 37 (1) (Jan. 2022) 81–93, https://doi.org/10.1109/TPWRS.2021.3090268.
[42] Arash Anzalchi, Arif Sarwat, Overview of technical specifications for grid-connected photovoltaic systems, Energy Convers. Manag. 152 (2017) 312–327, https://doi.org/10.1016/j.enconman.2017.09.049.
[43] X. Wu, J. Dai, Y. Tang, F. Xue, Adaptive under-frequency load shedding scheme for power systems with high wind power penetration considering operating regions, IET Gener., Transm. Distrib. 16 (2022) 4400–4416, https://doi.org/10.1049/gtd2.12609.
[44] U. Tamrakar, D.A. Copp, T. Nguyen, T.M. Hansen, R. Tonkoski, Optimization-based fast-frequency estimation and control of low-inertia microgrids, IEEE Trans. Energy Convers. 36 (2) (Jun. 2021) 1459–1468, https://doi.org/10.1109/TEC.2020.3040107.
[45] A.M. Jasim, B.H. Jasim, B.N. Alhasnawi, A. Flah, H. Kraiem, Coordinated control and load shifting-based demand management of a smart microgrid adopting energy internet, Int. Trans. Electr. Energy Syst. 2023 (2023), https://doi.org/10.1155/2023/6615150.
[46] M. Elshenawy, A. Fahmy, A. Elsamahy, S.A. Kandil, H.M. El Zoghby, Optimal power management of interconnected microgrids using virtual inertia control technique, Energies 15 (2022) 7026, https://doi.org/10.3390/EN15197026, 15, no. 19, p. 7026, Sep. 2022.